ABSTRACT

May, Shanna M. Gd^{3+}-Nitroxide Pairs for Protein-Membrane Studies: A Multifrequency EPR Approach
(Under the direction of Dr. Tatyana I. Smirnova)

The objective of this research project is to advance the well-established method of Site-Directed Spin Labeling (SDSL) Electron Paramagnetic Resonance (EPR) by utilizing many advantages that High Field EPR (HF EPR) could offer. Specifically, we propose to utilize nitroxide-Gd^{3+} label pairs for site-directed distance measurements in protein and protein-membrane structure studies. The proposed method is based on through space dipole-dipole interactions between Gd^{3+} ion positioned on the surface of the bilayer and a nitroxide label attached at the point of interest on the lipid molecule or membrane associated protein. The proposed labeling approach coupled with multifreqency EPR can provide information on Gd^{3+}-nitroxide distance, as well as orientation of Gd^{3+}. Experiments were conducted to investigate the mechanism of nitroxide-Gd^{3+} interactions in solutions of various viscosities at multiple magnetic fields (corresponding frequencies from 9.5 to 220 GHz) in order to determine relative contributions of dipole-dipole and exchange interactions in nitroxide-Gd^{3+} pairs at various viscosities and to elucidate the relaxation processes modulating the dipole-dipole interaction as a function of magnetic field. Applications for membrane and membrane protein studies are also discussed.

Gd^{3+}-Nitroxide Pairs for Protein-Membrane Studies: A Multifrequency EPR Approach

By

Shanna Marie May

A thesis submitted to the Graduate Faculty of
North Carolina State University
In partial fulfillment of the
Requirements for the degree of
Master of Science

Department of Chemistry

Raleigh

2004

Approved by:

_____ _____

_____
Chair of Advisory Committee

I dedicate this work to the most wonderful, supportive fiancé in the world –

Ryan Harrelson

And to my parents who have always encouraged me to strive to be the best and not to settle for anything less -

Roy & Sylvia May

BIOGRAPHY

SHANNA MARIE MAY was born to Roy and Sylvia May on January 30, 1979 in Lumberton, North Carolina. Shanna has a younger brother, Stephen, who is currently serving in the Navy at Norfolk, Virginia.

A love and appreciation of science and math developed at an early age. Shanna's mother, Sylvia, is a math and science teacher in the public school system of North Carolina. Shanna graduated Magna Cum Laude from Lumberton High School in 1997. She then attended the University of North Carolina at Pembroke where she intended to major in English and then attend law school. After taking freshman Chemistry as a desired elective, she immediately saw her calling and changed to a major in Molecular Chemistry.

Shanna graduated from the University of North Carolina at Pembroke with a degree in Molecular Chemistry in 2001. After doing research at UNCP and talking with mentors about different career opportunities, she enrolled in North Carolina State University in Raleigh in 2001.While in her first semester at NCSU, she became engaged to Mr. E. Ryan Harrelson.

While in graduate school, Shanna has thoroughly enjoyed her TA position and has found her niche in Physical Chemistry at NCSU. Shanna joined the EPR research group under the direction of Dr. Tatyana I. Smirnova at NCSU. Upon graduation, Shanna will be teaching college chemistry full time.

ACKNOWLEDGEMENTS

"I can do all things through Christ which strengtheneth me."
Philippians 4:13

First and foremost, I give the Lord the glory for this work. The Lord has been beside me and carried me throughout this work. Without Him, I would not have succeeded in this goal.

The Lord has truly blessed me with many people that have loved, guided, and encouraged me through this time in my life. I would like to acknowledge my fiancé, Ryan, for his never-ending love and support. He has always been there for me through thick and thin and always supported my work. He has been my best friend, my loyal companion, and loved me unconditionally through this time. I am honored and blessed to call him my fiancé and one day, my husband.

I would also like to acknowledge my parents and family. My parents, Roy and Sylvia May, have always made me strive for excellence by their example. They have instilled in me the knowledge of how to set goals and fulfill them. Without their unconditional love and support, I would not be who I am today. I love them for who they are and the example the show to others. I am honored to call them my parents. I would also like to mention my fiancés parents, George and Connie Harrrelson. As long as I have known them, they have always supported my goals and dreams. They have constantly supported Ryan and I in all our dreams and we have great respect for them. I am blessed to have such role models in my life. Thank you all.

I would also like to acknowledge some of my colleges here at NCSU. First of all, I would like the thank Lan Quan for being such a good friend. I would also like to thank

Shani Smith for always listening and offering a great word of encouragement. I would also like to thank Dr. Alex Smirnov and his research group. We always worked together and collaborated on the research so I felt as much his student as Dr. Smirnovas'. I would also like to thanks Andres Ruuge, who as a postdoctoral fellow in Dr. Smirnovs' research group, helped me tremendously with my questions and experimental designs. I would also like to thank NCSU Department of Chemistry for their financial support for the research.

The final person I would like to recognize is my advisor, Dr. Tatyana I. Smirnova. Tatyana has been a great advisor as well as friend. She has gone above and beyond the call of duty to make sure I understand the new theory and ideas behind the research I performed. She was not only a mentor but also a person I could confide in. She was a wonderful advisor and I will always be grateful for all the assistance, thoughtfulness, and honesty she brought to my research.

TABLE OF CONTENTS

LIST OF TABLES

LIST OF FIGURES

1 INTRODUCTION

Understanding the structure-function relationships in membrane and membrane-associated proteins is of fundamental importance for many reasons. First of all, functions of membrane proteins are of enormous physiological significance. Those functions include but are not limited to signal transactions, molecular and ion transport. Some of these proteins are known to operate as mechano-electrical switches in such diverse physiological processes as touch, hearing and osmotic regulation in bacteria. Many membrane proteins are promising targets for novel pharmaceuticals (1).

Most structures of membrane proteins determined up to date have been solved by X-ray crystallography (2-4). Membrane proteins can be reconstituted into 2-D membrane protein crystals in presence of lipids and analyzed by electron microscopy (EM). Recent developments in Nuclear Magnetic Resonance (NMR) have also provided impressive progress in membrane protein structure determination (5). Despite the advances, the Protein Data Base (PDB) contains the structure of only fifty membrane proteins, compared with many thousands of structures of water-soluble proteins. At the moment, determination of structures of membrane proteins represents a frontier in structural biology. Clearly, new experimental methods are needed that can assist in structure determination of membrane protein as well as to provide information on dynamics of membrane associated systems.

Recently, there has been a renewed interest in spin labeling Electron Paramagnetic Resonance (EPR) as a tool to investigate protein and peptide structure. Site-directed spin labeling (SDSL), developed by Hubbell and others (6), have made it possible to insert a

spin-labeled side chain by cysteine mutagenesis at a chosen site on a protein. Analysis of the continuous wave (CW) EPR spectrum of such a label can provide information on side chain dynamics, solvent accessibility, polarity, and the local electrostatic environment for the labeled residue probed. Obtaining this information for a systematic set of spin-labeled mutants help to determine protein topography, secondary structure, and some features of tertiary structure. SDSL EPR also can be used to measure distances within macromolecules. Structural information can be obtained by measuring distances between two paramagnetic centers in proteins.

The goal of this work is to develop a novel spin-labeling approach to allow us to use the advantages of High-Field EPR (HF EPR) to study membrane and membrane-associated proteins.

1.1 Site-Directed Spin-Labeling EPR

EPR combined with site-directed spin labeling (SDSL), which uses molecular biology to introduce new labeling sites has emerged as a powerful tool that can be used to determine the structure and dynamics of proteins and macromolecules (7).

Using spin labeling EPR for distance determination is advantageous since measurements may be carried out in disordered systems and physiologically relevant conditions (3). Most proteins are EPR silent and must be labeled with a paramagnetic probe using SDSL technique. The most common SDSL technique is reacting a site-directed cysteine mutant with a methanethiosulfonate nitroxide reagent to produce the side chain designated R1 (8), which is shown in Figure 1.

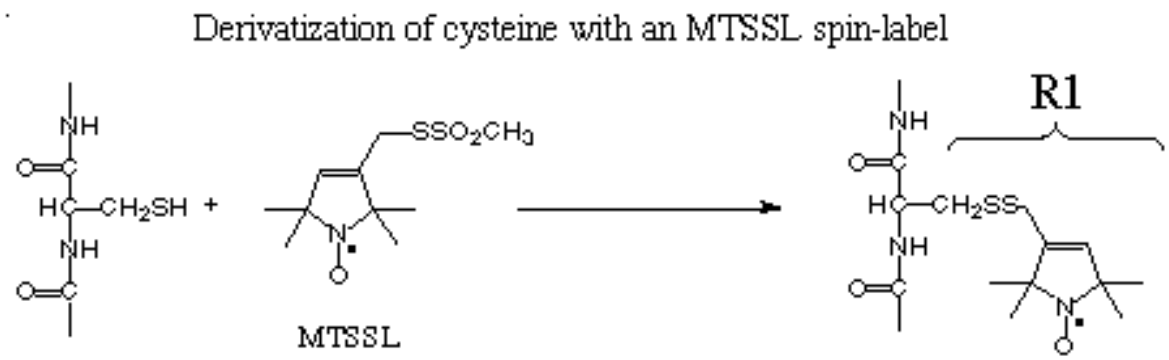

Figure 1: Chemical Modification of Cysteine with MTSSL (methanethiosulfate spin-label)

Distances can also be measured by EPR upon the addition of a second paramagnetic center and observing and analyzing magnetic interactions between the two paramagnetic centers under optimal conditions (9). Changes in interspin distance would produce large spectral changes, making it straightforward to monitor conformational changes in proteins (10). Typically, EPR spectra become broadened by dipolar or exchange interactions, which arise from pairs of interacting spins such as two nitroxides (10) or a nitroxide and a paramagnetic metal ion (7).

Solvent accessibility and mobility and local polarity of the side chain can be determined from the EPR spectrum when the protein is labeled with a single nitroxide. One could also determine the secondary structure by monitoring the local dynamics of the side chain (8).

1.2 Distance Measurements by EPR

The SDSL distance measurements within macromolecules are based on measuring magnetic interactions between a nitroxide and another paramagnetic label. One approach is to use another nitroxide as the second label (10). In some cases it is advantageous to use, as a relaxer, a paramagnetic metal ion that is either naturally present in the protein or attached to the protein through an engineered binding site (7). These two approaches will be discussed below.

1.2.1 Nitroxide-Nitroxide Interactions

As early as in 1967 Likhtenshtein and Bobodzhanov (11) developed an EPR method for studying the relative position and molecular movements of protein groups based on the specific chemical modification of these groups by derivatives of iminoxyl stable radicals and by complexes with paramagnetic metals. They used the method of double paramagnetic labels to distinguish three types of lysine groups in human serum albumin that are next to guanidine, histidine, and tyrosine groups respectively (11). Kulikov et al. (12) used the method of paramagnetic labels to determine the distances between the functional groups of proteins. They used the method to evaluate the distances between the functional groups in lysozyme (histidine, lysines), myoglobin (histidines), and myosin (sulphydryl groups). Their results for lysozyme and myoglobin were in satisfactory agreement with the X-ray structural models of the proteins (12).

More recently, Rabenstein and Shin (10) developed a method to determine the distance between two spin labels attached to a macromolecule. A series of ά-helical peptides, each modified with two nitroxide spin labels, were used to develop an EPR "spectroscopic

ruler" (10). In this method, the pure dipolar spectrum for two interacting spins in the frozen state is directly Fourier deconvoluted from the dipolar broadened continuous-wave EPR (CW-EPR) spectrum. The dipolar spectrum was then used to get the average interspin distance and the variance of its distribution. These dipolar spectra were used to estimate distances between two specifically placed nitroxides in the range of 8-25Å. This method accurately measures the interspin distance in this range. The major drawback of this EPR method was that it required for the sample to be frozen at ca. 100 K. Freezing of the sample is performed so the rotational diffusion of the spin pair would be sufficiently slow to prevent motional averaging of the interaction. Freezing the sample, however, eliminates the possibility of studying structural dynamics (7). It is also important to consider studying biological systems in their native state, which could be at room temperature.

1.2.2 Nitroxide-Metal Interactions

Voss et al. (7) developed an alternative approach based on metal-nitroxide interactions. They used molecular genetics to introduce both a metal binding site and a nitroxide spin label into the same protein. Theory for distance-dependent relaxation effects of metals such as Cu^{2+}, Mn^{2+}, or Gd^{3+} on a nitroxide in a rigid lattice system was presented by Leigh (13). Voss et al. applied Leigh theory to analyze the effect of Cu^{2+} on the EPR spectra of nitroxide spin-labeled side chains, that were introduced at three different distances from a designed metal ion binding site in T4 lysozyme (7). This study was of importance since it has shown that the distances could be determined under the rigid

lattice conditions in frozen solution. They also have shown when the labels are in restricted slow motion (that holds true for labels attached to large proteins at physiological conditions) use of Leigh approach introduces only minor error in distance determination (7).

Another approach was proposed in a study by Voss et al. (14) where the magnetic interactions between a nitroxide spin label and a paramagnetic Gd^{3+} ion were considered. The effect of Gd^{3+} sequestered by a chelator bound covalently to Cys residue on spin-labeled side chains at positions located at different positions was investigated. Gd^{3+} (ion spin state, S = 5/2) has a larger magnetic moment than Cu^{2+} (S = ½) that results in longer interspin distances that can be probed. Spectral broadening due to dipolar interactions between a Gd^{3+} ion and a nitroxide were analyzed using the Leigh model. The presence of Gd^{3+} reduces the spectral line height in each of the three mutants as a result of broadening (15). The range of calculated interspin distance values were from 15.8 – 23.7Å. The Gd^{3+}-spin-label distances determined by this method, were significantly longer than those estimated from nitroxide-nitroxide interactions between the same sites, probably, due to the nature of the Gd^{3+} chelator. Authors speculate that as a result of long attachment, the probes may assume many orientations with respect to the backbone, it is difficult to predict the direction and distance of the spin centers relative to the labeled side chain and that results in substantial error in distance determination (14).

1.3 Spin Labeling to Study Membrane and Protein-Membrane Interactions

Despite the fundamental importance of membrane proteins and other multi-component protein systems, only a few spectroscopic techniques lend themselves to study details of structural organization of these proteins in membranes and the role of molecular interactions with lipids. The slow-motional regime of membrane proteins makes high-resolution solution NMR methods impossible that are successful in structure determination of smaller water-soluble proteins. Membrane proteins are also difficult to crystallize, and therefore X-ray crystallography of membrane proteins remains a major challenge.

Over the years, EPR has been extensively used to study membrane-protein interactions and protein transmembrane structure. Typically for EPR experiments, the protein is first labeled at a desired site and then reconstructed in a phospholipid bilayer. The emersion depth of the nitroxide labeled site in a bilayer can be determined by measurements of differential accessibility of that label to broadening agents like nonpolar (O_2) and/or water-soluble paramagnetic reagents. Sensitivity of EPR spectra to the probe microenvironment is used to determine the mobility and polarity patterns that yield data on the structure of transmembrane protein segments (16).

1.3.1 Measurements of Differential Accessibility of Paramagnetic Broadening Agents to Labeled Site

EPR method of estimation of the immersion depth of a nitroxide label in the phospholipid bilayer is based on exchange interactions during collision of the nitroxide with paramagnetic probe soluble in the aqueous or lipid phases of the bilayer (17). Altenbach et al. used ten mutants of bacteriorhodposin, each containing a single cysteine residue

regularly placed along α-helix D and facing the lipid bilayer, derivatized with a nitroxide spin label (18). This method for depth determination requires use of two fast-relaxing paramagnetic species with finite but different solubilities in the lipid and aqueous phases. The collision rates of the nitroxide with nonpolar oxygen increase with the distance from the membrane interface. On the other hand, collisional rates with hydrophilic metal complexes decrease over the same distance. The logarithm of the ratio of the collision rate of oxygen to those of a polar metal ion complex, called the "depth parameter," has a linear dependence along the distance from the bilayer surface. By calibrating the depth parameter using the spin-labeled phospholipids with the known position of the label, one can determine the localization of the individual nitroxide relative to the plane of the phosphate groups in the bilayer. Accessibility parameter can also be analyzed as a function of the position of the nitroxide in the protein (this approach is known as a "nitroxide scan"). Periodicity in the accessibility parameter also reports on secondary structure of the transmembrane domains. For example, periodicity of 3.6 residues is characteristic of an α-helical structure, while periodicity of 2 residues is typical for a β-sheet fold. Additional information could be obtained by analyzing periodicity in mobility and polarity of spin-labeled sites. For example, mobility of the label on protein-lipid interface is expected to be restricted, while mobility of the label exposed to the inside cavity of a membrane channel or attached to mobile loops not participating in protein-membrane interaction will be less restricted. Altenbach et al. (18) performed a benchmark study to track accessibility of polar and nonpolar reagents and mobility patterns to identify surface residues and residues buried within a protein core. Thirty consecutive single cysteine substitution mutants of bacteriorhodopsin were prepared then

modified with a sulfhyfral specific nitroxide reagent. The accessibilities of the attached nitroxides to collisions with hydrophilic and hydrophobic paramagnetic probes in solution were determined and the EPR spectra were analyzed in terms of side chain mobility. This work has demonstrated that in the hydrophobic segments, both the accessibility and mobility data were consistent with helical structures.

1.3.2 Using Ni^{2+}-Nitroxide Interactions to Determine Membrane Protein Structure

Another approach, aimed to determine position of the labeled protein side-chain with respect to the membrane surface is based on labeling the bilayer with Ni^{2+}-chelating lipids that confine paramagnetic Ni^{2+} ions to the membrane interface has been reported in the literature (19). Interactions between magnetic Ni^{2+} and nitroxide attached to a protein side chain results in changes in nitroxide electronic relaxation. Because Ni^{2+} has such a short electronic relaxation time, it was concluded that the leading mechanism of enhanced nitroxide relaxation is the Heisenberg spin exchange, which is known to be the most efficient only for direct collisions assisted by lipid translational diffusion. It was shown that "Ni^{2+}-lipid" method is suitable to differentiate between spin-labeled chains near the membrane interface, but only if those belong to the protein-lipid contact surface. The relaxation enhancement diminished quickly toward the bilayer center, as one would expect because of the limited magnitude of the lipid diffusion and a short range of the spin exchange interaction. The enhancement was also low for the residues located close to the bilayer interface but buried inside the protein and also for those located deep in the bilayer. Another potential problem of this method is that in order to achieve a suitable

enhancement, one out of four lipids was labeled with a large chelating group containing Ni^{2+}. This could potentially interfere with the proper insertion of proteins in such a bilayer (19).

1.4 Analyzing Dipole-Dipole Interactions

Distance determination by EPR is based on observation of magnetic interactions between two spin labels. The main interactions are spin exchange and dipolar coupling. The exchange interaction, (J), arises from the overlap of the orbitals of unpaired electrons (17). Neighboring spins also experience local magnetic fields that are induced by their respective magnetic dipoles. In classical physics, the following expression describes the energy (U) of dipole-dipole coupling between two magnetic point dipoles ($\boldsymbol{\mu}_1$ and $\boldsymbol{\mu}_2$) which are separated by a distance r (where ($\boldsymbol{\mu}_1$, $\boldsymbol{\mu}_2$, and **r** are vectors) and μ_o is the permeability constant (15):

$$U = \frac{\mu_o}{4\pi}\left\{\frac{\vec{\mu}_1 \bullet \vec{\mu}_2}{r^3} - 3\frac{(\vec{\mu}_1 \bullet \vec{r})(\vec{\mu}_2 \bullet \vec{r})}{r^5}\right\} \qquad (1)$$

Using $\hat{\mu} = \gamma\hbar\hat{I}$ (where ħ =h/2π is Planck constant and I is the spin) and replacing the energy by the Hamiltonian operator:

$$\hat{H}_{dd} = \frac{\mu_o}{4\pi}\gamma_1\gamma_2\hbar^2\left\{\frac{\hat{I}_1 \bullet \hat{I}_2}{r^3} - 3\frac{\left(\hat{I}_1 \bullet \vec{r}\right)\left(\hat{I}_2 \bullet \vec{r}\right)}{r^5}\right\} \tag{2}$$

Where γ_1 and γ_2 are the gyromagnetic ratios of the two magnetic particles. The vector products can be written out and the spin Hamiltonian can be expressed as:

$$\hat{H}_{dd} = \frac{\mu_o}{4\pi}\frac{\gamma_1\gamma_2\hbar^2}{r^5}\begin{Bmatrix}\hat{I}_{1x}\hat{I}_{2x}\left(r^2-3x^2\right)+\hat{I}_{1y}\hat{I}_{2y}\left(r^2-3y^2\right)+\hat{I}_{1z}\hat{I}_{2z}\left(r^2-3z^2\right)\\-\left(\hat{I}_{1x}\hat{I}_{2y}+\hat{I}_{1y}\hat{I}_{2x}\right)3xy-\left(\hat{I}_{1y}\hat{I}_{2z}+\hat{I}_{1z}\hat{I}_{2y}\right)3yz-\left(\hat{I}_{1z}\hat{I}_{x}+\hat{I}_{1x}\hat{I}_{2z}\right)3zx\end{Bmatrix} \tag{3}$$

This equation can then be transferred into a matrix equation: $\hat{H}_{dd} = \vec{I}_1 \bullet D \bullet \vec{I}_2$ (4)

where $\vec{I}_1$ is a row vector, $\vec{I}_2$ is a column vector, and **D** is a matrix with elements D_{ij} (i,j=x,y,z). The matrix **D** (the dipolar coupling tensor) is then given by:

$$\hat{H}_{dd} = \left(\hat{I}_{1x}\hat{I}_{1y}\hat{I}_{1z}\right)\begin{pmatrix}D_{xx} & D_{xy} & D_{xz}\\ D_{yx} & D_{yy} & D_{yz}\\ D_{zx} & D_{zy} & D_{zz}\end{pmatrix}\begin{pmatrix}\hat{I}_{2x}\\ \hat{I}_{2y}\\ \hat{I}_{2z}\end{pmatrix} \tag{5}$$

Matrix theory defines that the trace of a matrix is invariant for a rotation in space. Also, it is easy to show that the trace of **D** is zero:

$$Tr(D) = \sum_i^i D_{ij} = (r^2-3x^2)+(r^2-3y^2)+(r^2-3z^2) = 0 \tag{6}$$

If motion is isotropic, all positions of **r** in space have an equal probability and the average value of tensor **D** can be found by calculating the average values of the elements D_{ij} if motion is fast. It is found that the average tensor **D** vanishes for fast isotropic rotational diffusion (tumbling) and it is a traceless tensor. As a result, dipolar interaction does not contribute to the Hamiltonian that determines the positions of the lines in magnetic resonance spectra. Spin-spin exchange coupling is different from dipolar interaction (dipole-dipole). J-coupling typically works through the electrons in bonds while the dipolar interaction is a direct interaction through space. J is isotropic and the contribution of the spin-spin coupling is independent of magnetic field. Spin exchange interactions occur in solutions of free radicals where collisions occur so that an overlap. In addition, the J-coupling tensor is not traceless. As a result, even in solution, J-coupling is observed. In the solid state, dipolar coupling is observed and its value is large leading to extensive signal broadening. In solution, the dipolar interaction is not observed due to the rapid and isotropic tumbling of the molecules and the fact that the trace of the dipolar coupling tensor is zero (15).

1.4.1 Relaxation Induced by Dipolar Interactions

Terms causing spin-lattice relaxation lead to an uncertainty in the transition quantities and hence to the line broadening (15). This implies a non-secular contribution to T_{2dd}^{-1}, equal to ½ T_1^{-1}. The dipolar term also modulates the energy levels directly, leading to a secular contribution to line widths and T_{2dd}^{-1} which depends on the zero-frequency spectra density J(0). The full equation for T_{2dd}^{-1} is

$$T_{2dd}^{-1} = \frac{1}{40}(2\pi R)^2\left[4(J) + J(\omega_x - \omega_A) + 3J(\omega_A) + 6J(\omega_X) + 6J(\omega_X + \omega_A)\right] \qquad (7)$$

where R is defined below, ω_A and ω_X are the appropriate Larmor frequencies); which, for a single-exponential correlation function is

(8)

$$\frac{1}{T_{2dd}} = \gamma^4\hbar^2 S(S+1)\frac{\tau_c}{r^6}\left[4 + \frac{1}{1+(\omega_X - \omega_A)^2\tau_c^{\,2}} + \frac{3}{1+\omega_A^{\,2}\tau_c^{\,2}} + \frac{6}{1+\omega_x^{\,2}\tau_c^{\,2}} + \frac{6}{1+(\omega_x + \omega_A)^2\tau_c^{\,2}}\right]$$

where τ_c is the correlation time.

The corresponding equations for $T_{1\rho dd}^{-1}$ (in the limit $B_1 \to 0$) are

$$T_{1\rho dd}^{-1} = \frac{1}{40}(2\pi R)^2\left[4J(\Omega_1) + J(\omega_x - \omega_A) + 3J(\omega_A) + 6J(\omega_X) + 6J(\omega_X + \omega_A)\right] \qquad (9)$$

$$T_{1\rho dd}^{-1} = \frac{1}{20}(2\pi R)^2\tau_c\left[4 + \frac{1}{1+(\Omega_1)^2\tau_c^{\,2}} + \frac{1}{1+(\omega_x - \omega_A)^2\tau_c^{\,2}} + \frac{3}{1+\omega_A^{\,2}\tau_c^{\,2}} + \frac{6}{1+\omega_x^{\,2}\tau_c^{\,2}} + \frac{6}{1+(\omega_x + \omega_A)^2\tau_c^{\,2}}\right] \qquad (10)$$

In the previous equations, Ω_1 is the strength of the radio frequency magnetic field, expressed in angular frequency units for a spin of magnetogyric ratio, γ, where ($\Omega_1 = \gamma B_1$). The factor R is proportional to:

$$R = (\mu_o / 4\pi)\gamma^2(\hbar / 2\pi)r^{-3}. \quad (11)$$

In the above formula, μ_o is the permeability constant, $\hbar = h/2\pi$ is Planck constant, and r is the interspin distance.

1.4.2 Leigh Method

Leigh described a model of three interactions between two unlike spins that is applicable to the dipolar interaction of a paramagnetic metal ion with a nitroxide for the case of the spin pairs in a rigid lattice. Leigh method is based on the original Redfield theory approach (13). The Redfield theory is only valid when the correlation time (τ_c) of the process modulating the dipole-dipole interaction is shorter than the reciprocal of the dipole interaction strength in frequency units (when $\tau_c < (\gamma_e H_z)^{-1}$, and H_z is the maximum dipolar field at the nitroxide. In the Leigh model, τ_c is equal to T_{1e}, the electronic relaxation time of the metal. The theory predicts an angular dependent line width of the nitroxide spectrum:

$$\delta H = C(1 - 3\cos^2 \theta_{R'})^2 + \delta H_o, \quad (12)$$

where the dipolar interaction constant, C, is:

$$C = \frac{g\beta\mu^2\tau}{hr^6} \quad (13)$$

(g is the electronic g-factor of the nitroxide, β is the Bohr magneton, μ is the magnetic moment of the metal, r is the interspin distance, and δH_o is the line width in the absence of interaction. The angle $\theta_{R'}$ is between the interspin vector and the applied magnetic field. Because the interspin vector has a distribution of angles in the nitroxide coordinate frame, the spectral simulation involves an integration carried over the allowed range of $\theta_{R'}$ according to:

$$L(H) = \int_0^{2\pi}\int_0^{\pi}\int_0^{2\pi} L(\theta,\phi,\theta_r,H)\sin\theta\sin\theta_r d\theta d\phi d\theta_r \tag{14}$$

with L(θ,φ,H) is the individual component line shape as a function of orientation.
where L is the Lorentzian line shape function:

$$L = \frac{\delta H}{((H - H_m)^2 + \delta H^2)} \tag{15}$$

and the center positions of the resonance lines are given by:

$$H_m = \frac{\hbar\omega}{\beta g(\theta,\phi)} - \frac{A(\theta,\phi)m}{\beta g(\theta,\phi)} \tag{16}$$

Where m takes all the values of the nuclear quantum number of nitrogen, and

$$g(\theta,\phi) = (g_x{}^2 c_x{}^2 + g_y{}^2 c_y{}^2 + g_z{}^2 c_z{}^2)^{1/2},$$

$$A(\theta,\phi) = \frac{(A_x{}^2 g_x{}^2 c_x{}^2 + A_y{}^2 g_y{}^2 c_y{}^2 + A_z{}^2 g_z{}^2 c_z{}^2)^{1/2}}{g(\theta,\phi)},$$

where (17)

$$c_x = \sin\theta\cos\phi$$
$$c_y = \sin\theta\sin\phi$$
$$c_z = \cos\theta$$

This approach is commonly used to estimate the distances from the nitroxide label to the paramagnetic metal site. First, powder spectra are simulated from the equations above for a range of C, and the normalized amplitudes of the central line ($m_I = 0$ resonance) (I/I_o) are plotted verses the dipolar interaction coefficient normalized to the natural line width ($C/\delta H_o$), where I/I_o is given by:

$$\frac{I}{I_o} = \frac{(I/I_o)_o - (I/I_o)_\infty}{1 + (C/\delta H_o / k^{1/2})^p} + \frac{|I|}{|I_o|_\infty} \qquad (18)$$

Using this calibration plot, experimental values of I/Io (determined as a ratio of amplitude of the central line in presence of the paramagnetic relaxer to the amplitude of this line in the absence of the relaxer) and line width are used to determine C, from which the interspin distance, *r*, is determined (13).

2 PROPOSED APPROACH

2.1 Motivation to Use Gd^{3+}-Nitroxide Pairs for Membrane Studies and Distance Measurements

Our method is based on spin-label relaxation enhancement by through-space dipolar interactions between a nitroxide and paramagnetic Gd^{3+} ions that are positioned at the membrane interface by binding to chelating lipids. Specifically, it is proposed to manipulate the Gd^{3+} electronic relaxation by changing the magnetic field: electronic relaxation of Gd^{3+} slows with the increasing magnetic field strength. Slow (as compared with other paramagnetic metal ions) electronic relaxation of Gd^{3+} at magnetic fields above 3 T and the highest possible for an ion spin state (S = 7/2) would result in easily observable relaxation enhancement effects for the labels located at either side of the bilayer surface. In addition, at high magnetic fields, EPR spectra from many spin-labeled peptides and proteins approach slow motional regime in which all three principal axis components of the g-matrix become clearly resolved allowing measurements of anisotropic relaxation enhancement. This can provide not only the distances between the nitroxide and the bilayer surface but also the orientation of the nitroxide with respect to that surface. Contributions from the Heisenberg exchange, that complicate data analysis for nitroxide-nitroxide or nitroxide-copper pairs at short (<10 Å) distances, are likely to be negligible for shielded unpaired electronic spins of Gd^{3+}. At X-band (9.4 GHz, 0.3 T) typical EPR spectra of Gd^{3+} complexes are rather broad (300 - 500 G) and as such do not affect analysis of much narrower nitroxide spectra. The electronic relaxation of Gd^{3+} in

aqueous solutions is unusually slow compared to other lanthanide ions at magnetic fields of conventional X-band EPR (0.3 T, 9.5 GHz). We propose that because T_{1e} for Gd^{3+} could be shorter than the typical rotation correlation time of the interspin vector (0.6 ns), the dipole-dipole interaction could be primarily modulated by the T_{1e} of the Gd^{3+} complex. Depending on the experimental needs, T_{1e} could be further attenuated by varying the chelate structure used to attach Gd^{3+}. For long-range distance measurements one would wish to slow Gd^{3+} electronic relaxation even further and this can be achieved by increasing the magnetic field of the experiment. As the magnetic field increases, T_{1e} of Gd^{3+} increases dramatically, reaching >30 ns at around 3.4 T for some complexes (20). Magnetic field dependence of T_{1e} for Gd^{3+} complexes provides a unique way to increase the magnitude of dipole-dipole correlation time responsible for the changes in EPR spectra — specifically, to move the experiments to higher magnetic fields. There is a possibility that at typical HF EPR fields (3-5 T), the electronic relaxation of Gd^{3+} can become longer than the correlation time of the interspin vector rotation so that the interspin rotational correlation time would modulate the dipole-dipole interactions. (This time determines the range of measurable distances in nitroxide-nitroxide experiments at room temperature.) However, in the case of Gd^{3+}, the S(S+1) factor would cause a 21-fold increase in the magnetic moment vs. that of a nitroxide (S = ½). If this dipolar field is partially averaged by rotations, then the range of measurable distances is increased by a factor of $(21)^{1/6}$ =1.66 by use of Gd^{3+}. In high field EPR experiments, the EPR spectrum of Gd^{3+} is separate from the nitroxide spectra and can be analyzed independently of the nitroxide. At frequency 95 GHz and higher, the x, y, and z components of g-tensor of the

nitroxide are spectrally resolved and can provide a way to study the anisotropy of Gd^{3+}-nitroxide interactions.

3 EXPERIMENTAL APPROACH

3.1 Understanding Gd^{3+}-Nitroxide Magnetic Interactions

In order to use Gd^{3+}-nitroxide interactions for distance measurements, we have to understand the mechanism of relaxation enhancement and determine process that modulates the Gd^{3+}-nitroxide dipole-dipole interactions. The goal of this part of the project is to determine relative contributions of Heisenberg exchange and dipolar interactions in nitroxide relaxation enhancement upon addition of Gd^{3+} and to elucidate the process responsible for modulating dipole-dipole interactions under various experimental conditions. To do that, the effect of Gd^{3+} ions on T_2-relaxation time of nitroxide radical was investigated in liquids of various viscosities and in frozen samples as a function of magnetic field.

3.1.1 Methods

Sample Preparation. Gadolinium complexes of 1,4,7,10-tetraazacyclododecane-N-(n-pentyl)-N'-N''-N'''-tri-acetic acid (Gd^{3+}-DTPA) (Figure 2), 3,6,9-triaza-3,6,9-tris(carboxymethyl)-4-(4-ethoxybenzyl)undecandicarboxylic acid (Gd^{3+}-EOB-DTPA) (Figure 3), and $Gd(NO_3)_3$-$6H_20$ were prepared. The Gd^{3+}-DTPA and Gd^{3+}-EOB-DTPA

were provided by Schering AG, Germany, and used without further purification. The $Gd(NO_3)_3$-$6H_20$ was purchased from Aldrich, Milwaulkee, WI. Concentration of aqueous stock solution of Gd^{3+}-DTPA was 66mM. Concentration of aqueous stock solution of Gd^{3+}-EOB-DTPA was 100 mM. Concentration of aqueous stock solution of $Gd(NO_3)_3$-$6H_20$ was 50 mM. Concentration of aqueous stock solution of $La(NO_3)_3$ was 50 mM. The same pH was maintained upon addition of Gd^{3+} complexes by using 200mM Hepes buffer, pH = 5.6 (Hepes purchased from Sigma, St. Louis, MO). PDT (perdeuterated TEMPO) (Figure 4) was purchased from ISOTECH, Miamisburg, OH and 40 mM PDT stock was prepared. Glycerol was purchased from Fisher Scientific Company (Fairlawn, NJ) and a 75% glycerine/buffer stock solution was prepared. For model experiments, varying concentrations (0, 2.25, 4.5, 6.75, 9, 11.25, and 13.5 mM) of the Gd^{3+} complexes in 200 mM Hepes buffer, 5mM PDT, 50/50 Hepes buffer/glycerol, were prepared.

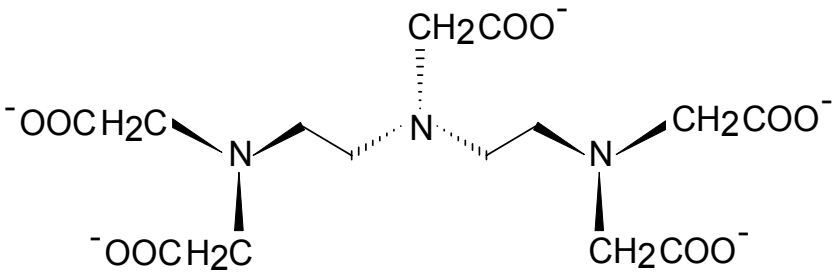

Figure 2: Structure of DTPA chelator used in this work.

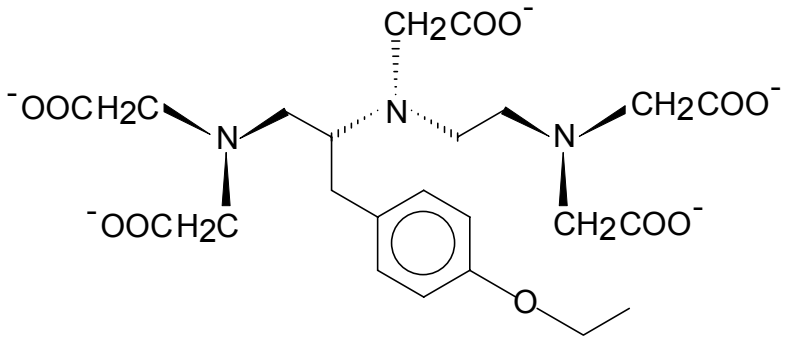

Figure 3: Structure of EOB-DTPA chelator used in this work.

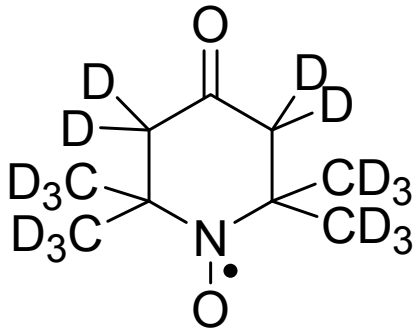

Figure 4: PDT structure

X-band Measurements. To obtain 9.5 GHz CW EPR spectra, solutions were drawn into a gas-permeable poly(tetrafluoroethylene) (PTFE) capillaries (Zeus Industrial Products Inc., NJ), the ends were closed by folding, and the capillary was placed inside a standard EPR quartz tube (3 mm internal diameter (i.d.)) open at both ends. The tube was fixed inside the variable-temperature dewar of the X-band resonator. Samples were

deoxygenated in the EPR cavity by continuous flow of nitrogen gas around the gas-permeable capillary-containing sample. For measuring concentrational dependence of PDT EPR signal on Gd^{3+} complexes, X-band EPR spectra of PDT were acquired at 10 ^{o}C, 19 ^{o}C, and also frozen with liquid nitrogen. A Varian (Palo Alto, CA) Century Series E-109 X-band spectrometer was equipped with a Varian TE102 cavity and a Varian temperature controller. Temperature was measured with a miniature T-type thermocouple fixed next to the sample capillary and a Barnant microprocessor-based thermocouple thermometer (Barnant Company, IL). Stabilization of the gas flow in addition to fixed positions of sample and thermocouple sensor in the dewar insert significantly improved temperature stability of the sample. Temperature was stable and repeatable within +/- 0.5 ^{o}C from measurement to measurement. Spectra were taken with modulation amplitude 0.5 G over magnetic field scan of 100 G.

High Frequency 95 GHz and 220 GHz Measurements. High-frequency W-band (95 GHz) EPR measurements were performed at the Florida State University in Tallahassee using a Bruker Elexsys 680 FT/CW spectrometer with a Hybrid3 magnet system equipped with an E680 console. Samples were drawn into quartz capillaries with i.d = 0.2 mm. Temperature was maintained using an Oxford variable temperature system. Temperature was stable and repeatable within +/- 0.5^{o}C.

Spectral Simulations. To extract line broadening (T_2-broadening of frozen samples) induced by the presence of a paramagnetic relaxer, from continuous-wave EPR spectra,

inhomogenously broadened EPR spectra of nitroxide labels were simulated under a one-line-width-parameter model:

$$F(B) = \int_{-\infty}^{+\infty} F_0(B')m(B - B')dB' \tag{19}$$

Where $F_o(B)$ is the spectrum taken in the absence and $F(B)$ in the presence of a relaxer, and $m(B)$ is the broadening measured as $\delta(\Delta B^L_{p\text{-}p})$ (20). Broadening function $m(B)$ can be a Lorentzian or a Voight function (convolution of Lorentzian and Gaussian functions).

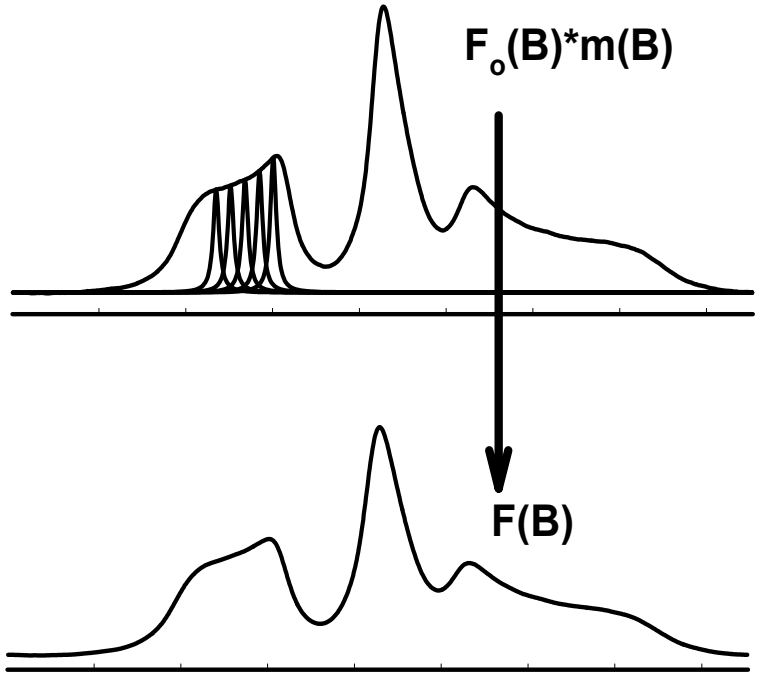

Figure 5: Least-squares fitting with one-line-width –parameter broadening model where: $F_o(B)$ is the spectrum taken in absence of a relaxer; $F(B)$ is the spectrum in the presence of a relaxer; $m(B)$ is the Lorentzian broadening measured (21)

Spectra of nitroxide in liquid solutions were simulated as a superposition of three Lorentzian functions to extract line widths of each of three nitroxide hyperfine components and magnitude of hyperfine coupling constant. All spectral simulations were done using program package "Ewvoigt" from Scientific Software Services, Plymouth, MI.

3.1.2 Results and Discussion

3.1.2.1. Contribution of Heisenberg Exchange

Addition of Gd^{3+} complexes or Gd^{3+} salts to nitroxide radicals in solutions results in shortening of both T_1 and T_2 relaxation times of the nitroxides. The T_2 relaxation enhancement can be measured by CW EPR experiments as line width broadening of a nitroxide signal. Figure 6 shows typical 9.5 GHz CW EPR signal from 5 mM PDT in 50%w/w buffer-glycerol mixture in the presence of 11.25 mM Gd-DTPA. The experimental spectrum is superimposed with the best-fit result using three Lorentzian lines. Residual (difference between experimental spectrum and fit) demonstrates the good agreement between experiment and simulation, with the residual showing only small deviations at the center of the signal. These deviations may be caused by the effects of poorly resolved hyperfine interactions with remote deuterons, or by instrumental effects of modulation on very narrow line of PDT. Lorentzian line width of each of the three nitrogen hyperfine components (for m_I = -1, 0 ,1) is plotted as a function of Gd-DTPA concentration in Figure 7. The dependence is linear and is characterized by slopes of 47, 46.5, and 46.5 mG/mM for each of the three lines.

Two mechanisms can contribute in line width broadening of nitroxide EPR signal in the presence of paramagnetic Gd^{3+} ion: Heisenberg exchange and dipole-dipole spin-spin interaction. Heisenberg exchange requires direct overlap of electron wave functions of two species upon collision, which is very unlikely to be substantial for well-shielded d-electrons of Gd^{3+}. To demonstrate this experimentally we have measured line width broadening of nitroxide radical induced by gadolinium nitrate and by two different gadolinium complexes: Gd-DTPA and Gd-EOB-DTPA. Chelation of gadolinium with large group like DTPA would substantially decrease electron overlap upon collision with nitroxide and result in decrease of the exchange contribution to the line width. Even more convincing proof could be obtained in experiment with La^{3+} ions. La^{3+} is known to have extremely fast electronic relaxation. As a result, line width broadening induced by dipole-dipole interactions is negligibly small and all broadening effects should be attributed to Heisenberg exchange interaction. Figure 8 shows 9.5 GHz CW EPR signal from 5 mM PDT in 50%w/w buffer-glycerol mixture in the presence of 11.25 mM $La(NO_3)_3$.

Figure 9 shows dependence of the line width of the EPR signal from 5 mM PDT solution in 50/50 (w/w) glycerol/Hepes buffer at T = 23 ^oC for three nitroxide components as a function of lanthanum nitrate concentration. Because we expected very small broadening effect, or no effect at all, we have used 10 times higher concentrations of lanthanum than corresponding concentrations of gadolinium used in this work. The dependence is linear with an average slope of -0.3 mG/mM, essentially zero (Figure 9). Similar results were obtained in experiments carried out at a magnetic field of 3.3 T using W-band spectrometer. Virtually no measurable effect of lanthanum on the PDT line width was

detected upon addition of up to 150 mM. Figure 10 shows the effect of the addition of gadolinium nitrate on EPR line width of PDT radical in 50% buffer/glycerol solution as measured with an X-band spectrometer. The relaxation enhancement effect is 44 mG/mM for gadolinium nitrate (Figure 11). The magnitude of this effect is the same as upon the addition of Gd-EOB-DTPA complex (39 mG/mM) (Figure 12), demonstrating that chelating of Gd^{3+} ion with bulk groups does not affect the magnitude of the broadening. These results support our hypothesis that no measurable contribution to the EPR line width of PDT signal can be observed from Heisenberg exchange interaction between the nitroxide and the gadolinium spins. The absence of Heisenberg exchange interaction in proposed labeling pair is advantageous, since no correction for this effect will be needed in distance calculations.

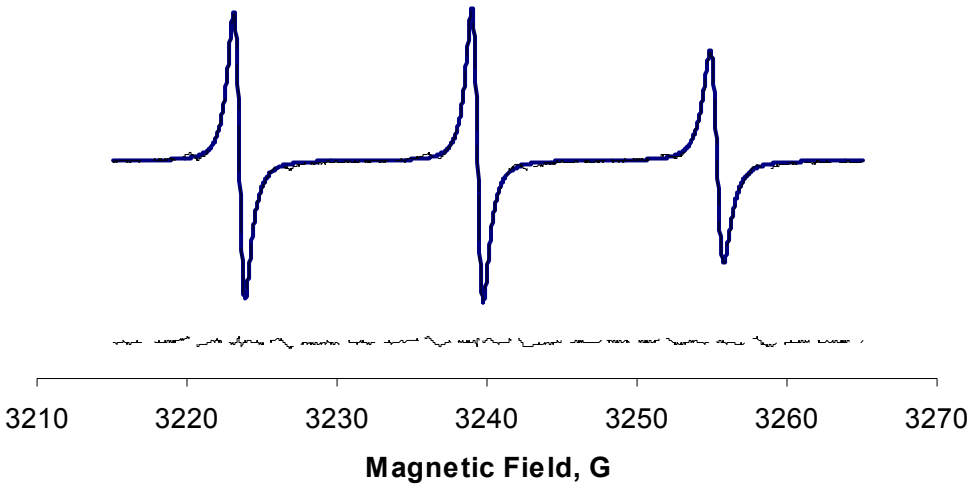

Figure 6: 9.5 GHz experimental spectrum (dashed line) of 5mM PDT in the presence of 11.25 mM Gd-DTPA, 50/50 (w/w) glycerol/Hepes buffer, T = 10 ^{o}C is superimposed with the best fit (solid line) using three Lorentzian lines. The residual is shown below.

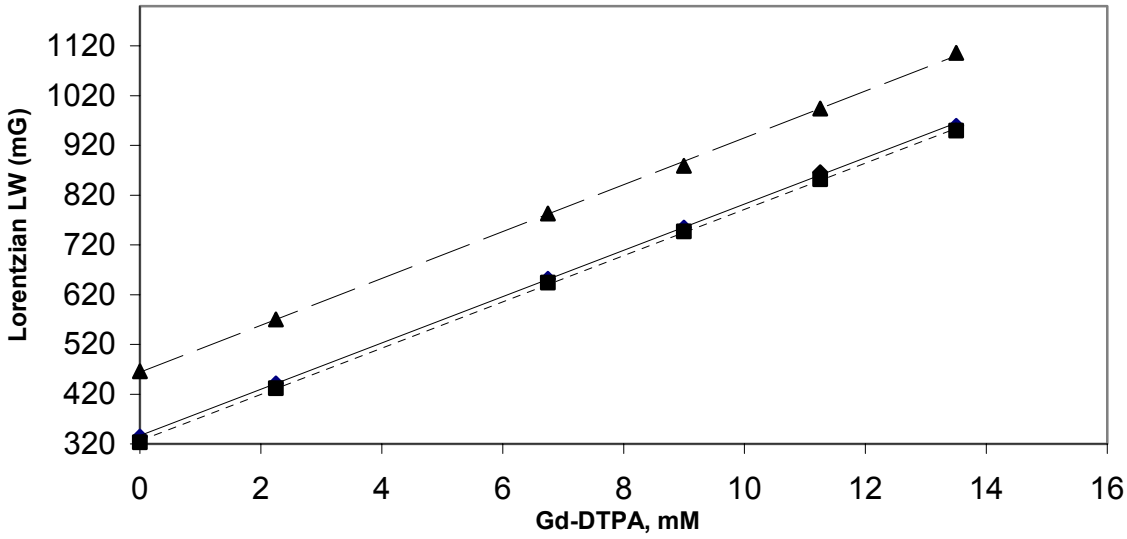

Figure 7: 9.5 GHz Lorentzian peak-to-peak line width of three nitroxide hyperfine components of PDT as a function of Gd-DTPA concentration, T = 10^{o}C, 50/50 (w/w) glycerol/Hepes buffer. Bottom line shows low field (-1), top line shows high field (+1) and middle line shows central field (0) components.

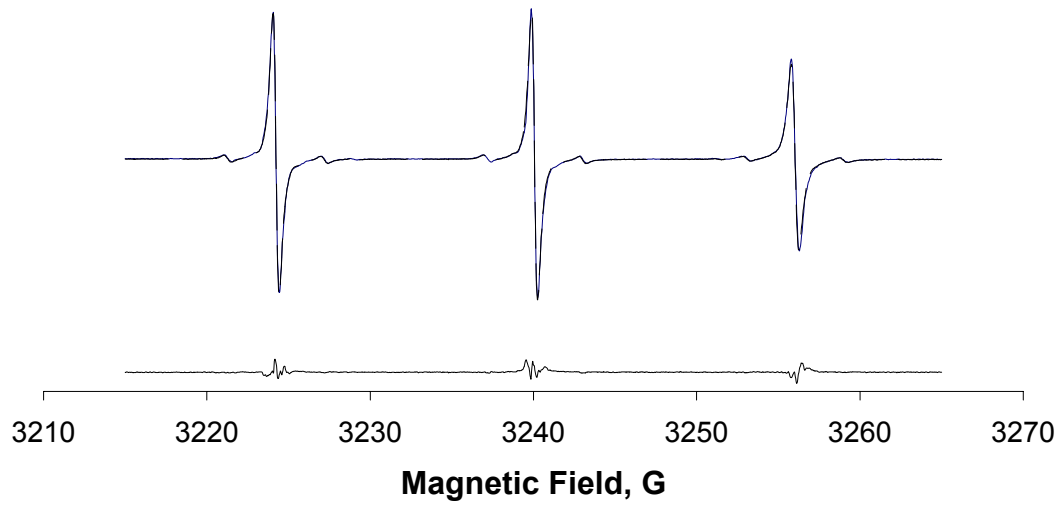

Figure 8: 9.5 GHz experimental spectrum (dashed line) of 5mM PDT in presence of 11.25 mM $La(NO_3)_3$, 50/50 (w/w) glycerol/Hepes buffer, T = 23^{o}C is superimposed with the best fit (solid line) using three Lorentzian lines. The residual is shown below.

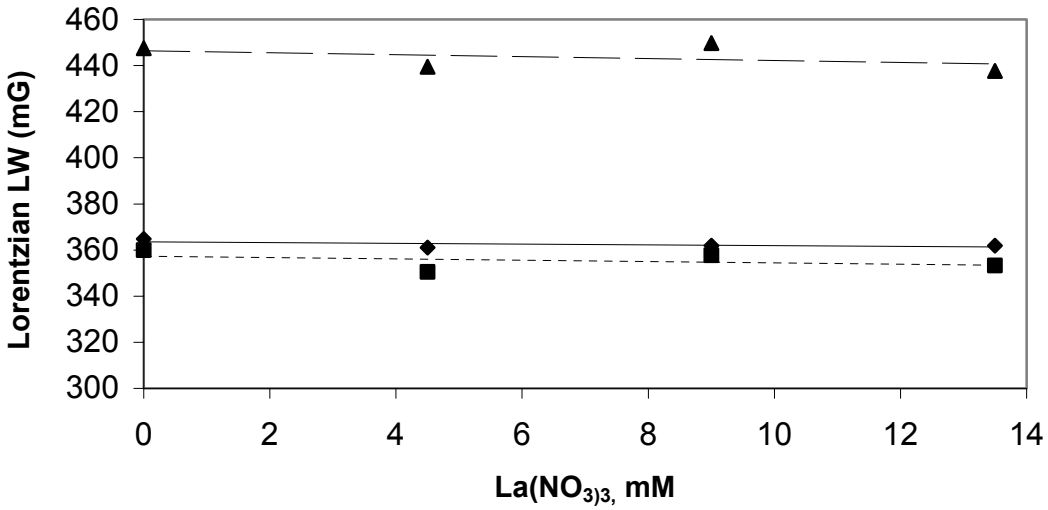

Figure 9: 9.5 GHz Lorentzian peak-to-peak line width of three nitroxide hyperfine components of PDT as a function of $La(NO_3)_3$ concentration, T = 23 ^oC, 50/50 (w/w) glycerol/Hepes Buffer. Bottom line shows low field (-1), top line shows high field (+1) and middle line shows central field (0) components.

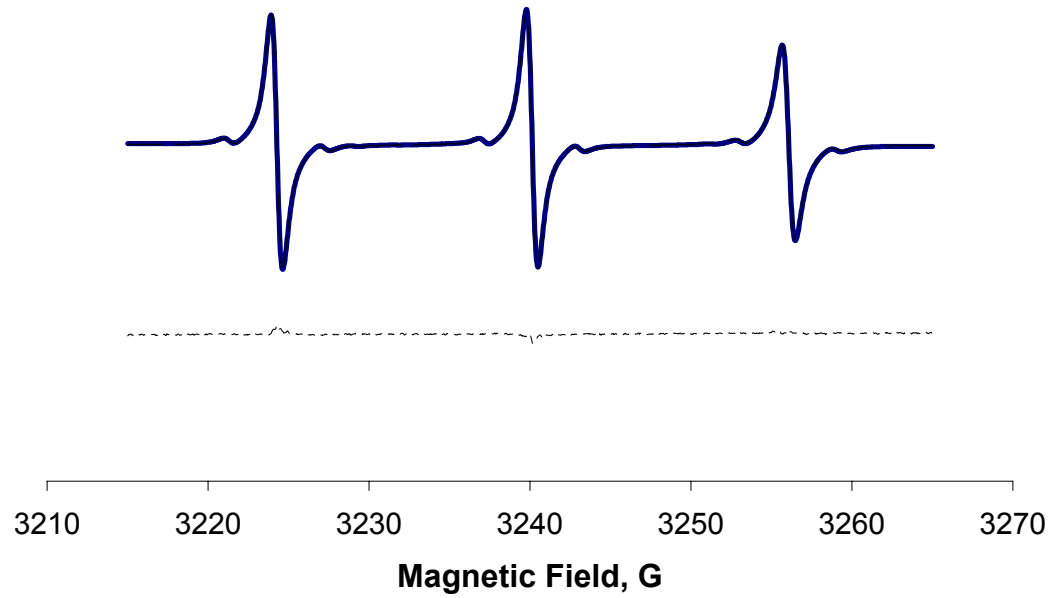

Figure 10: 9.5 GHz experimental spectrum (dashed line) of 5mM PDT in presence of 11.25 mM $Gd(NO_3)_3$, 50/50 (w/w) glycerol/Hepes buffer, T = 19^oC is superimposed with the best fit (solid line) using three Lorentzian lines. The residual is shown below.

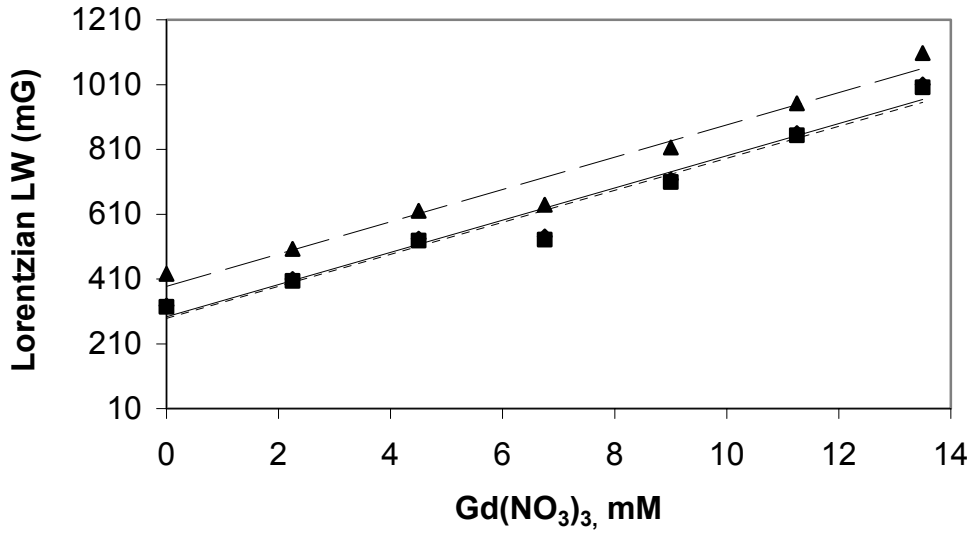

Figure 11: 9.5 GHz Lorentzian peak-to-peak line width of three nitroxide hyperfine components of PDT as a function of $Gd(NO_3)_3$ concentration T = 19°C, 50/50 (w/w) glycerol/Hepes Buffer. Bottom line shows low field (-1), top line shows high field (+1) and middle line shows central field (0) components.

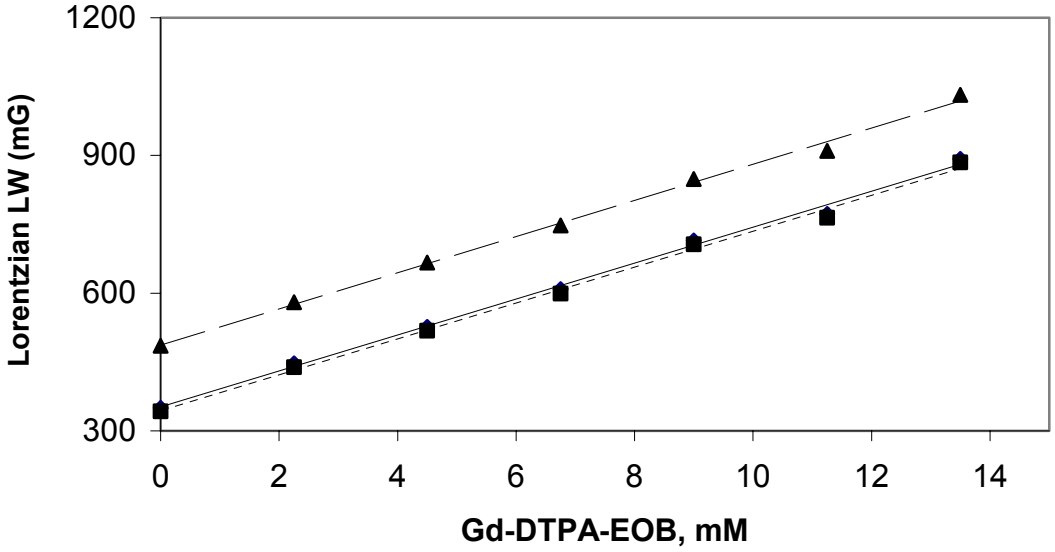

Figure 12: 9.5 GHz Lorentzian peak-to-peak line width of three nitroxide hyperfine components of PDT as a function of Gd-DTPA-EOB concentration T = 10°C, 50/50 (w/w) glycerol/Hepes Buffer. Bottom line shows low field (-1), top line shows high field (+1) and middle line shows central field (0) components.

3.1.2.2 Investigation of Dipole-Dipole Interactions

To answer the question - what process modulates the dipole-dipole interaction (T^2_{dd}) in nitroxide-Gd pairs observed through a nitroxide EPR spectrum, we have to consider three processes: the rotational motion of the interspin vector between nitroxide and Gd^{3+}, with respect to the external magnetic field, the change in the length of the interspin vector, and T_1 electronic relaxation of Gd^{3+}. The fastest of the four processes would then modulate the dipole-dipole interaction and the rate of that process would determine correlation function and τ_c in equation 8. The electronic relaxation of Gd^{3+} in aqueous solutions at magnetic fields of conventional EPR (0.3 T) is estimated to be 0.3-1 ns (20). This relaxation rate is too fast to be measured directly in pulse EPR experiments and is usually estimated from NMR proton relaxation enhancement experiments. Specifically, for T_1 electronic relaxation time Gd-DTPA in aqueous solutions at room temperature and magnetic field of 0.3 T two values are reported in the literature: 0.3 ns (22) and 0.64 ns (20). These estimates are model dependent and should be taken with a certain degree of caution. Very little information is available on magnetic field dependence of T_{1e} of Gd^{3+} complexes. Based on available literature data, T_{1e} for Gd^{3+} could be shorter than the typical correlation time of the interspin vector (either rotational or translational) in viscous solutions and our working hypothesis is that, the dipole-dipole interaction could be primarily modulated by the T_{1e} of the Gd^{3+} complex.

If the dipole-dipole interaction is modulated by the electronic relaxation of Gd^{3+}, observed relaxation enhancement, measured as nitroxide line width broadening, will show magnetic field dependence, since T_{1e} increases with an increase in the magnetic

field. There should be no magnetic field dependence of the line width broadening if the dipole-dipole is modulated by the rotation of the interspin vector or by changes in the length of the interspin vector, since both depend upon relative translational motion of two spins with respect to each other. The latter diffusion processes are independent upon magnetic field strength. We can vary the correlation time of the interspin rotation or translation vector by changing the viscosity of the solution either by changing the temperature of the experiment or by using increasing viscosity by adding glycerol. If dipole-dipole interactions are modulated by the motion of interspin vector, Gd^{3+} induced nitroxide line width broadening should show temperature and viscosity dependence. Here we have to add that the electronic relaxation time of Gd^{3+} shows no temperature dependence in physiologically relevant range of temperatures.

To check our hypothesis we have investigated temperature and magnetic field dependence of the nitroxide linewidth broadening by Gd^{3+} complexes. For our experiments we have chosen 50 % w/w glycerol/buffer solution as a model environment since motion of the interspin Gd^{3+}-nitroxide vector in such solution is definitely faster the interspin correlation time for the Gd^{3+}-nitroxide pair attached to a protein (typical rotational correlation time for a small protein is of the order of a few nanoseconds and would be even longer for membrane proteins).

3.1.2.2.1 Effect of Temperature on Nitroxide Relaxation Enhancement

Changing the temperature of the experiment alters macro-viscosity of the buffer-glycerol mixture. The temperature dependence of the viscosity of the water-glycerol solutions is available in the literature. However, in our experiments we have used a very high concentration of buffer (200 mM) that could change the macro-viscosity of the water-glycerol solution and its temperature dependence. We have considered it advantageous to use spectroscopic methods to measure the effect of micro-viscosity so that we can obtain information directly from the EPR spectrum of PDT.

In the fast motional limit, the homogeneous line width of each hyperfine component of nitroxide free radical (T_2^{-1} or ΔB^L_{p-p}) can be expressed a function of nitrogen nuclear spin number (m_I):

$$T_2^{-1} = A + Bm_I + Cm_I^2 \qquad (20)$$

Where A, B, and C are the line width parameters, which can be expressed in terms of spectral densities and magnetic parameters of the radical and rotational diffusion tensor (23, 24, 25, 26). According to the fast motional theory, parameter B is proportional to the rotational correlation time (τ_c) of the nitroxide probe used in the system. Parameter B could be calculated as a half difference of line widths of high field and low field hyperfine components of the nitroxide spectrum. Parameter A is a line width of the central component of the nitroxide spectrum which, in addition to spectral densities arising from rotational modulation, contains contributions from magnetic spin-spin interactions. By monitoring the parameter B, we can monitor how the rotation of the nitroxide changes. Since rotational diffusion of the nitroxide depends upon the viscosity of the solution, changes in parameter B can be related to the changes in micro-viscosity

of the system. If the broadening from the Gd^{3+} is independent upon the translational motion of the particles in the system, the slope of A vs. B should be the same in the presence and in the absence of Gd^{3+}, with A shifted to the higher values by the magnitude of the Gd^{3+} broadening. If broadening is dependent on motion of the spins, the shift in A would vary upon temperature resulting in a slope of A vs. B being different in the presence and the absence of the broadening agent. Figure 13 shows spectral parameter A as a function of spectral parameter B as measured for 5 mM PDT in 50/50 buffer-glycerol solution at X-band in the absence (dashed line) and in the presence (solid line) of 9 mM Gd-DTPA. The line width parameters were determined from experimental X-band spectra taken over the temperature range –28.4 ^{o}C to 10.5 ^{o}C. The slopes of the lines in the linear region were found to be 0.57 and 0.58 in the absence and the presence of broadening agent, respectively. Those values are essentially the same within the experimental error. No temperature dependence of Gd^{3+} induced broadening was also observed for another gadolinium complex, Gd-EOB-DTPA. The line width parameters of nitroxide spectrum as measured at X-band over the temperature range –33.7 ^{o}C to –8.7 ^{o}C (linear range of A vs. B dependence) for 5 mM PDT in the presence of Gd^{3+}-EOB-DTPA are shown in Figure 14. The slopes of A vs. B were determined to be 0.5 in the absence and 0.5 in the presence of 9 mM of Gd-EOB- DTPA, showing no dependence of relaxation enhancement upon viscosity of the solution.

Experiment with Gd-EOB-DTPA was repeated at magnetic field 3.3 T (W-band). Results are shown in Figure 15. No temperature dependence of Gd^{3+} induced relaxation was observed at this magnetic field. The above results prove that in the range of magnetic field 0.3 to 3.3 T, the dipole-dipole interaction between nitroxide radical and

gadolinium complex in 50/50 buffer-glycerol solution is modulated by T_{1e} electronic relaxation of Gd^{3+} which remains faster than the translational or rotational motion of interspin vector in the investigated range of magnetic field.

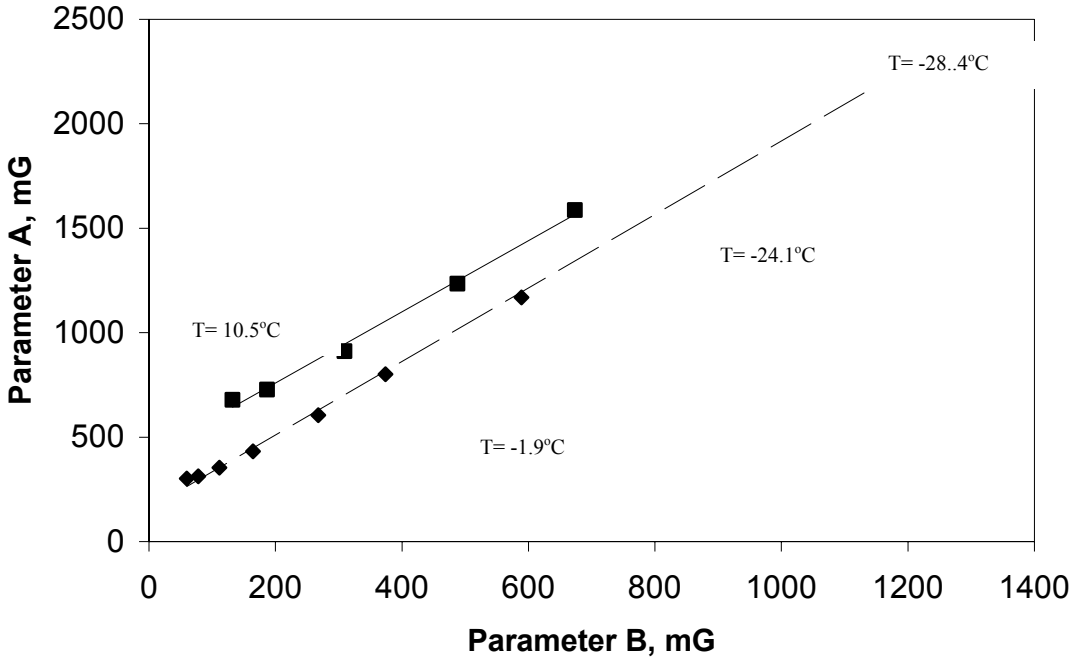

Figure 13: Comparison between A and B line width parameters calculated from 9.5 GHz EPR spectra of 5mM PDT (50/50 (w/w) glycerol/Hepes buffer) (squares) and in presence of 9 mM Gd-DTPA (triangles) in temperature range 10.5 ^{o}C to –28.4 ^{o}C.

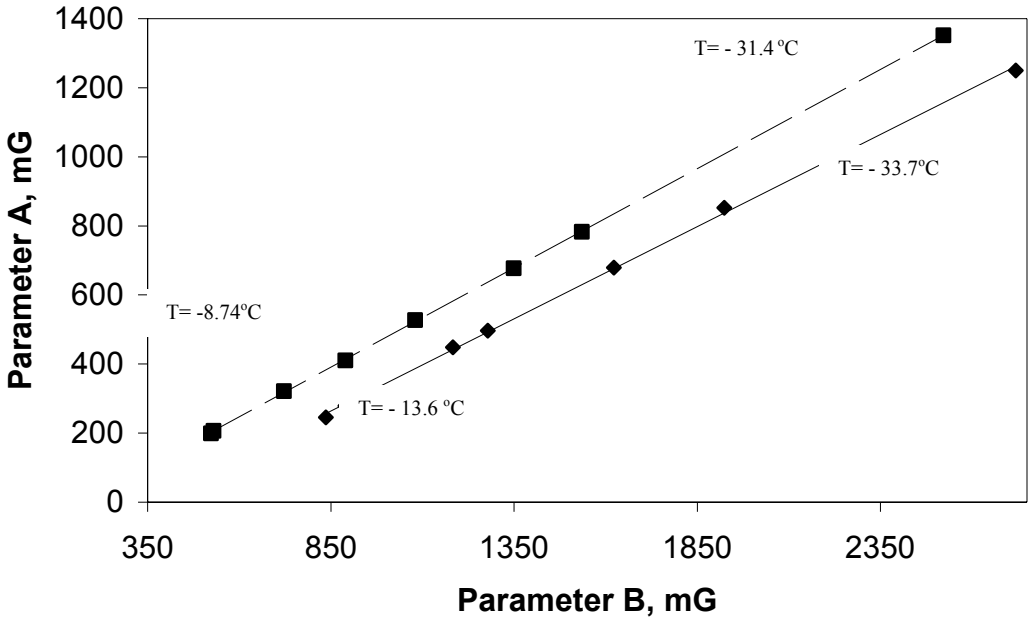

Figure 14: Comparison between A and B line width parameters calculated from 9.5 GHz EPR spectra of 5mM PDT (50/50 (w/w) glycerol/Hepes buffer) (squares) and in presence of 9 mM Gd-DTPA-EOB (triangles) in temperature range –8.7 ^{o}C to –33.7 ^{o}C.

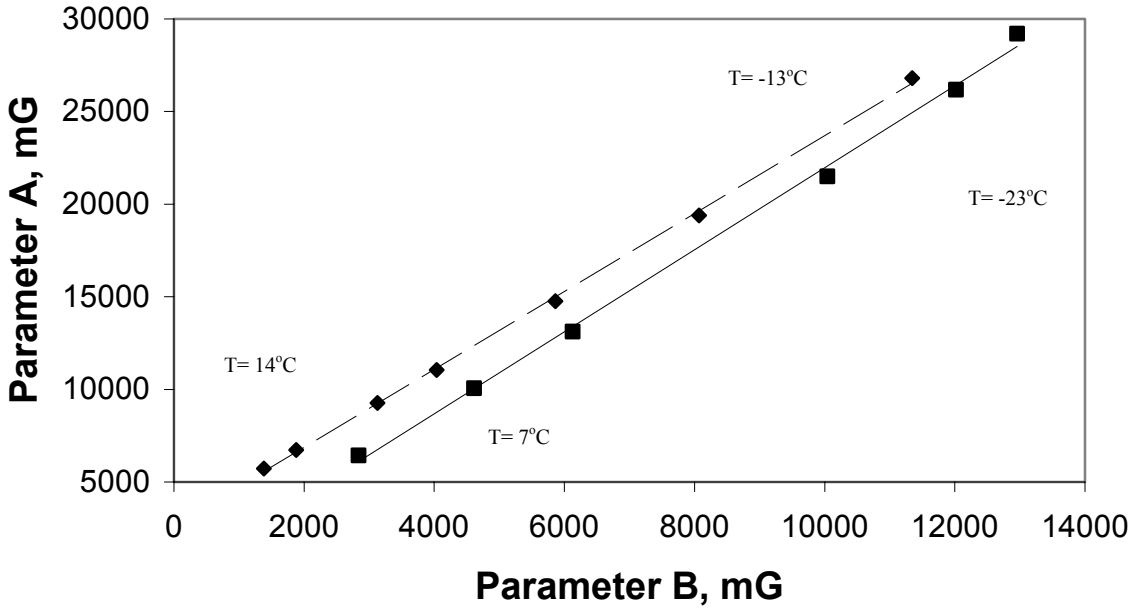

Figure 15: Comparison between A and B line width parameters calculated from 95 GHz EPR spectra of 5mM PDT (50/50 (w/w) glycerol/Hepes buffer) (squares) and in presence of 9 mM Gd-DTPA (triangles) in temperature range 14 ^{o}C to –23 ^{o}C.

3.1.2.2.2 Effect of Solution Viscosity on Gd^{3+}- Induced Relaxation Enhancement

Changing the solution viscosity at constant temperature by varying glycerol content of the solution would also alter conditions for interspin diffusion. We have investigated Gd^{3+} induced line width broadening in non-viscous aqueous solution. Line width of three hyperfine components of PDT in Hepes buffer as a function of gadolinium complex

concentration is shown on Figure 16 for Gd-DTPA and on Figure 17 for $Gd(NO_3)_3$. The magnitude of relaxation enhancement by Gd-DTPA in buffer was determined to be 52 mG/mM at 10 ^{0}C, compared to 47 mG/mM of Gd-DTPA in 50/50 buffer-glycerol solution. For gadolinium nitrate, the relaxation enhancement in buffer was determined to be 47 mG/mM at 19 ^{0}C, compared to 44 mG/mM in 50/50 buffer-glycerol solution at the same temperature (Table 1). The increase in slope, although small (it would translate into maximum of 41 mG broadening on the highest 13.5 mM concentration of gadolinium), is larger then expected experimental error in measurements of line width broadening at X-band. At first, these observations appear to show effect of the viscosity of the solution on the dipole-dipole interaction at X-band and to contradict our observation of no effect of micro viscosity of the solution in variable temperature experiments. However, careful analysis of sample preparation can explain the observed difference in relaxation enhancement for buffer and buffer-glycerol mixtures. To prepare samples, the appropriate amounts of stock solutions of PDT and Gd^{3+} complexes in buffer were mixed with required volume of buffer or the same volume of 75 %w/w buffer-glycerol mixture. Mixing the buffer and stock solutions does not result in change of the density of the mixture, while mixing the same ratio of buffer and 75 % w/w buffer/glycerol mixture results in a measurable change of density. Basically, even if we mix the same volumes of stock solutions in those two experiments, the resulting volume of buffer sample is smaller than the final volume of 50/50 buffer-glycerol mixture, resulting in volume concentration of Gd^{3+} complex being higher in buffer samples than in 50/50 buffer-glycerol samples. As a result, slopes of broadening versus Gd^{3+} concentration appears to be higher in experiments with buffer than in experiments with

50/50 buffer-glycerol mixtures. If correction for partial densities of solutions would be made (about 5%) the differences in slopes observed in buffer and buffer-glycerol mixtures would fall within the experimental error.

The absence of any effect of viscosity of the solution on the relaxation enhancement process proves that the dipole-dipole interaction under our experimental conditions is modulated by spin-lattice (T_{1e}) electronic relaxation.

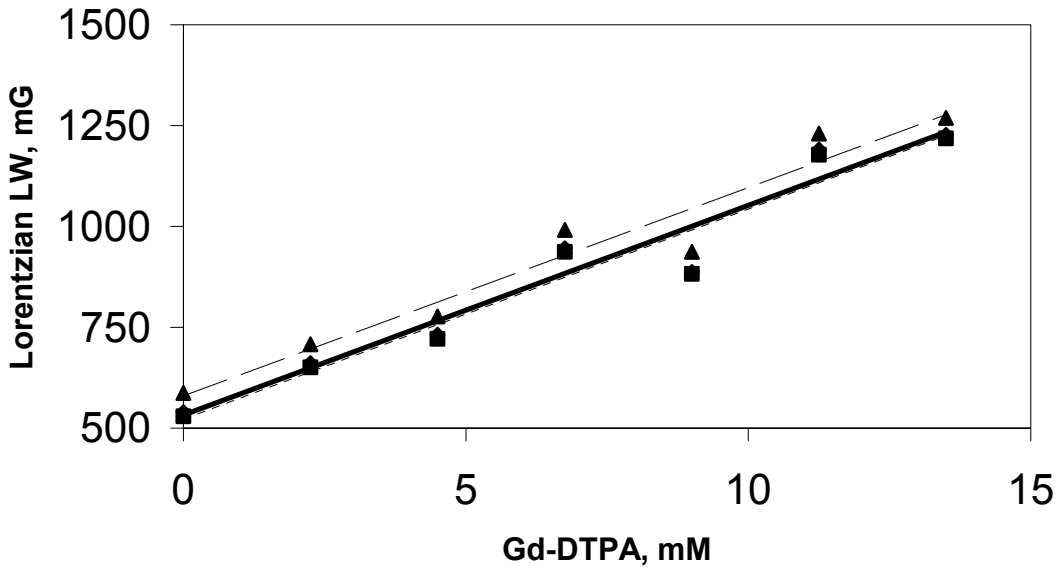

Figure 16: 9.5 GHz Lorentzian peak-to-peak line width of three nitroxide hyperfine components of PDT as a function of Gd-DTPA concentration, T = 10 ^{o}C, Hepes Buffer. Bottom line shows low field (-1), top line shows high field (+1), and middle line shows central field (0) components.

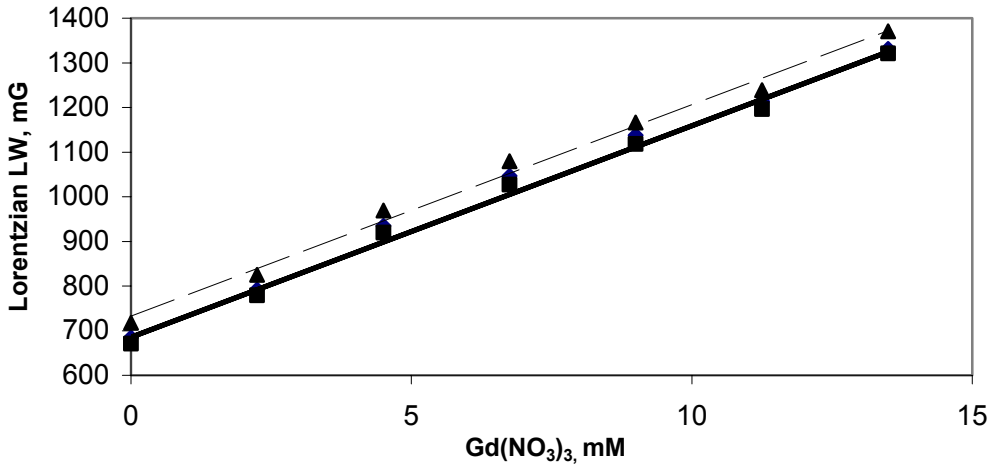

Figure 17: 9.5 GHz Lorentzian peak-to-peak line width of three nitroxide hyperfine components of PDT as a function of $Gd(NO_3)_3$ concentration T = 19 ^oC, Hepes Buffer. Bottom line shows low field (-1), top line shows high field (+1) and middle line shows central field (0) components.

Table 1: Average Lorentzian line width broadening and nitrogen isotropic hyperfine constants for PDT in various solvents and as a function of concentration of Lanthanide and Gadolinium ions

Broadening Agent / Solvent	Temperature (^{o}C)	Average Lorentzian broadening (mG/mM)	Nitrogen-hyperfine (G)	Frequency (GHz)
Gd-DTPA & 50/50 w/w glycerol/Hepes Buffer	10	47	15.9	9
Gd-DTPA & Hepes Buffer	10	52	15.9	9
Gd-DTPA & 50/50 w/w glycerol/Hepes Buffer	10	83	15.9	95
Gd-DTPA & 50/50 w/w glycerol/Hepes Buffer	10	84	15.9	220
Gd-EOB-DTPA & 50/50 w/w glycerol/Hepes Buffer	10	39	15.8	9
Gd-EOB-DTPA & 50/50 w/w glycerol/Hepes Buffer	19	43	15.8	9
Gd-EOB-DTPA & 50/50 w/w glycerol/Hepes Buffer	19	73	15.8	95
Gd-EOB-DTPA & 50/50 w/w glycerol/Hepes Buffer	19	112	15.8	220
$Gd(NO_3)_3$ & 50/50 w/w glycerol/Hepes Buffer	19	44	15.9	9
$Gd(NO_3)_3$ & Hepes Buffer	19	47	15.9	9
$La(NO_3)_3$ & 50/50 w/w glycerol/Hepes Buffer	23	-0.3	15.9	9

3.1.2.2.3 Effect of Magnetic Field on Gd^{3+}-Induced Nitroxide Relaxation Enhancement

Experiments described in the previous sections show conclusively that the dipole-dipole interaction between Gd^{3+} and nitroxide spins is modulated by spin-lattice (T_{1e}) electronic relaxation of Gd^{3+}. Now we can test our hypothesis that slowing down the electronic

relaxation of Gd^{3+} by conducting the experiments at higher magnetic fields would increase the magnitude of the Gd^{3+} induced nitroxide broadening. Figure 18 shows the line width of three nitrogen hyperfine components of the PDT EPR signal as a function of concentration of Gd-DTPA as measured at 95 GHz (magnetic field 3.3 T) and Figure 19 shows results of measurements at 220 GHz (magnetic field 8 T). The magnitude of the nitroxide relaxation enhancement increases from 47 mG/mM at 0.3 T to 83 mG/mM at 3.3 T to 84 mG/mM at 8 T. Figures 20 and 21 show results of multifrequency EPR experiment using Gd-EOB-DTPA. For this complex the magnitude of relaxation enhancement increases from 43 mG/mM at 0.3 T to 73 mG/mM at 3.3 T to 112 mG/mM at 8 T. Figure 22 shows how broadening induced by Gd-DTPA and Gd-EOB-DTPA changes with the varying magnetic fields (from 9 GHz to 220 GHz). The observed increase in nitroxide relaxation enhancement reflects slower T_{1e} electronic relaxation of Gd^{3+} at higher magnetic fields. The correlation time in equation 8 which we have proven to be the T_{1e} electronic relaxation of Gd^{3+} increases, resulting in a larger magnitude of dipole-dipole broadening. According to equation 8, this dependence is not linear, since we have to keep in mind that τ_c also contributes to a number of terms in brackets, which have inverse dependence on τ_c.

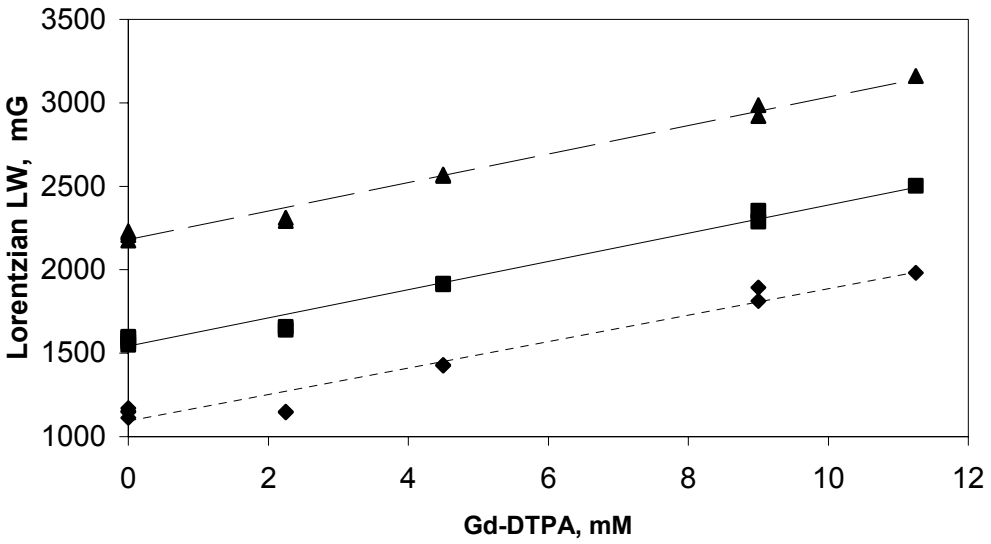

Figure 18: 95 GHz Lorentzian peak-to-peak line width of three nitroxide hyperfine components of PDT as a function of Gd-DTPA concentration, T = 10 ^{o}C, 50/50 (w/w) glycerol/Hepes Buffer. Bottom line shows low field (-1), top line shows high field (+1) and middle line shows central field (0) components.

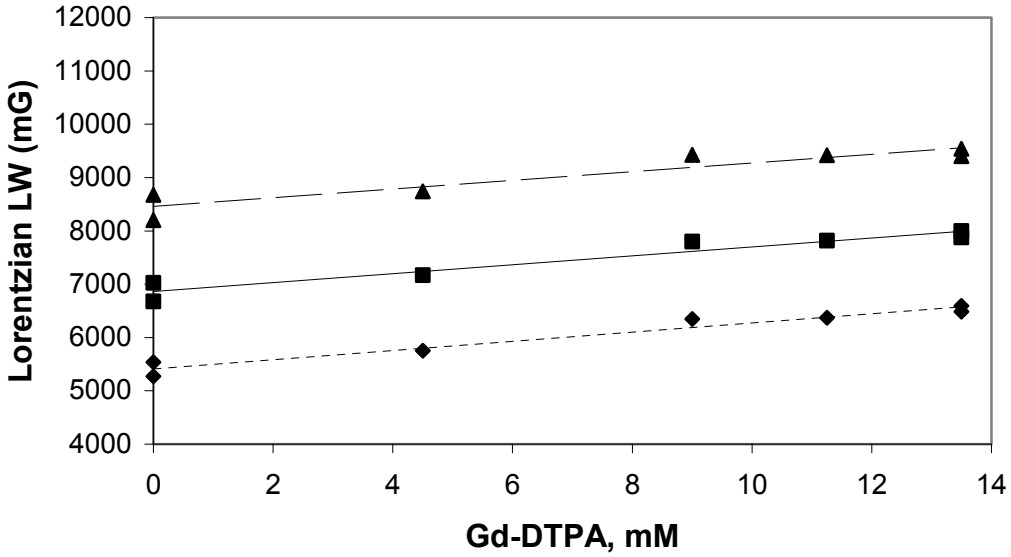

Figure 19: 220 GHz Lorentzian peak-to-peak line width of three nitroxide hyperfine components of PDT as a function of Gd-DTPA concentration, T = 10 ^{o}C, 50/50 (w/w) glycerol/Hepes Buffer. Bottom line shows low field (-1), top line shows high field (+1) and middle line shows central field (0) components.

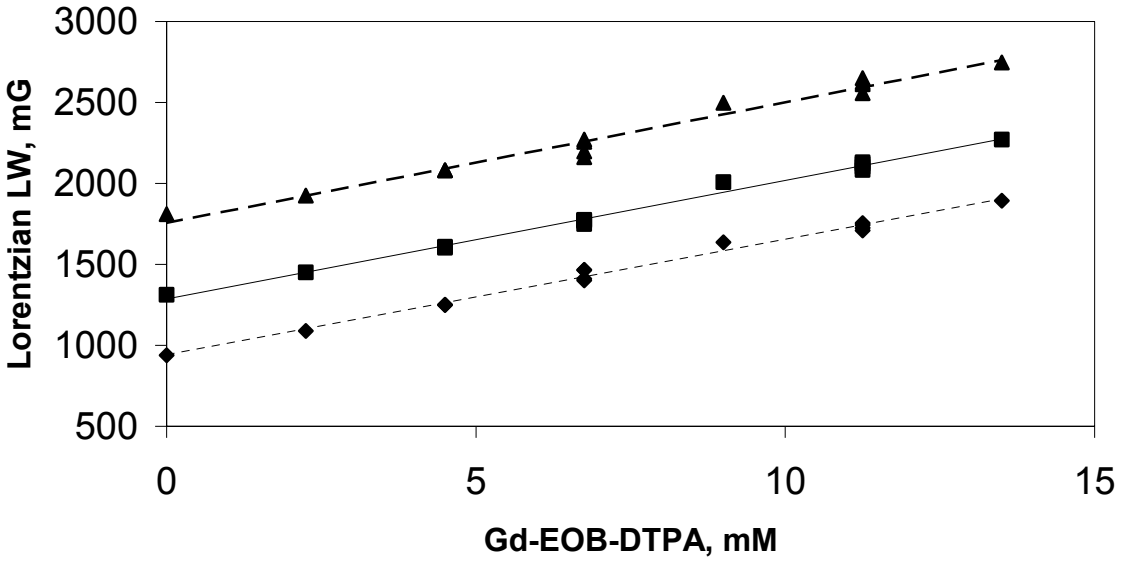

Figure 20: 95 GHz Lorentzian peak-to-peak line width of three nitroxide hyperfine components of PDT as a function of Gd-DTPA-EOB concentration 50/50 (w/w) glycerol/Hepes Buffer, T = 19 ^{o}C. Bottom line shows low field (-1), top line shows high field (+1) and middle line shows central field (0) components.

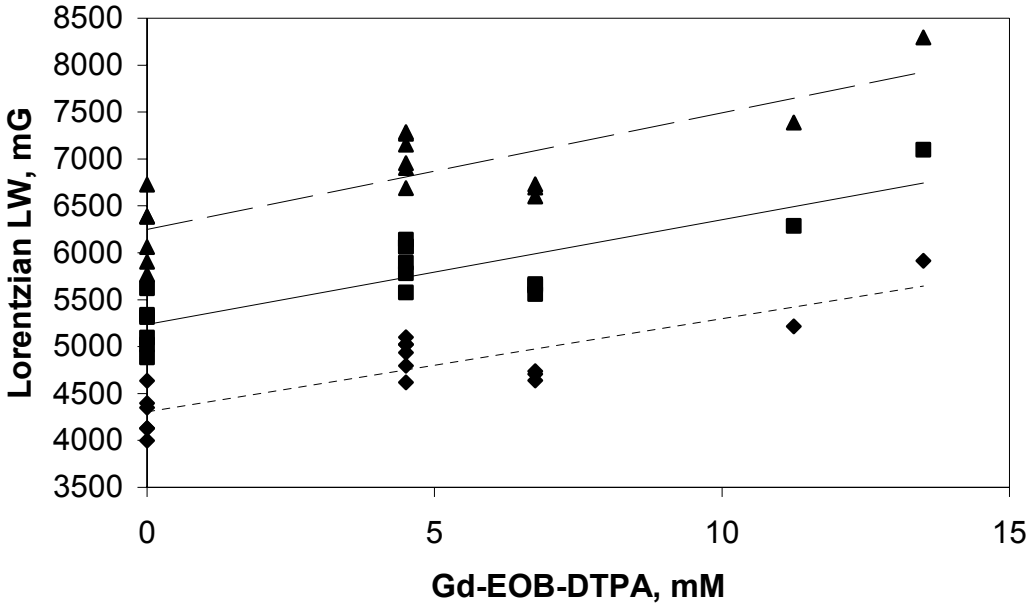

Figure 21: 220 GHz Lorentzian peak-to-peak line width of three nitroxide hyperfine components of PDT as a function of Gd-DTPA-EOB concentration 50/50 (w/w) glycerol/Hepes Buffer, T = 19 ^{o}C. Bottom line shows low field (-1), top line shows high field (+1) and middle line shows central field (0) components.

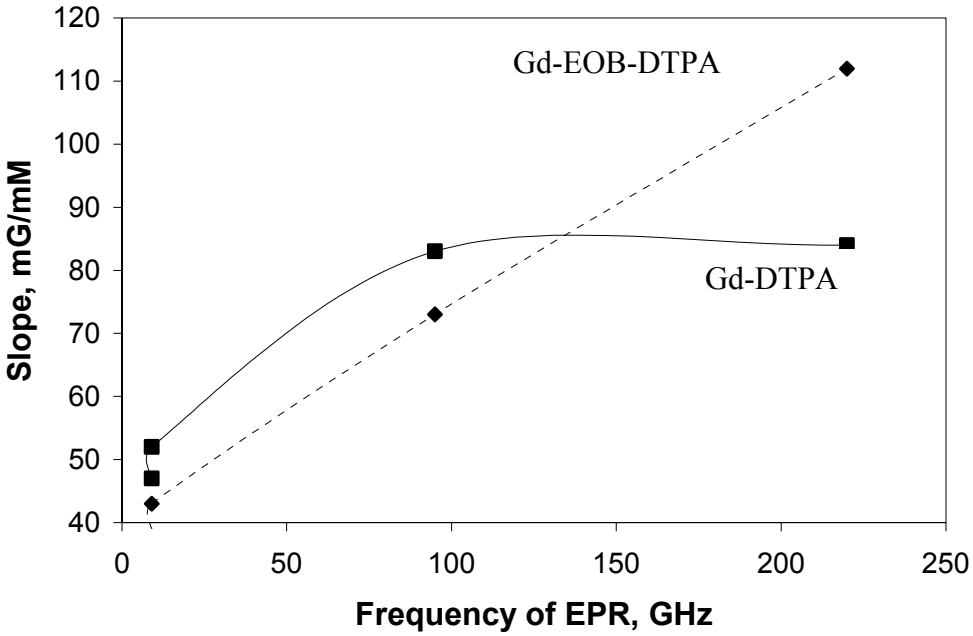

Figure 22: Plot of how broadening induced by Gd-DTPA (squares) and Gd-EOB-DTPA (triangles) changes with the varying frequencies of EPR experiments (from 9 GHz to 220 GHz)

3.1.2.2.4 Conclusions From Model Solution Studies

Results of experiments reported above allow us to make the following conclusions:

1) For moderately viscous aqueous solutions of nitroxide radicals, Heisenberg exchange contribution to the nitroxide relaxation enhancement by the Gd^{3+} complexes measured as line width is negligibly small when compared with the dipole-dipole

contribution, so dipolar theory should be used for distance determination and consideration for spin exchange is not required.

2) Nitroxide-Gd^{3+} dipolar interaction under conditions studied is modulated by spin-lattice T_{1e} electronic relaxation of Gd^{3+}.

(3) Magnetic field dependence of spin-lattice T_{1e} electronic relaxation of Gd^{3+} could be used to modulate the magnitude of Gd^{3+}-induced line width broadening. Specifically, longer interspin distances could be measured at higher magnetic fields.

3.2 Using Gd^{3+}-Nitroxide Pairs to Label Model Phospholipid Bilayers

The goal of this part of the project is to introduce the use of Gd^{3+}-nitroxide pairs for membrane protein studies. In order to position Gd^{3+} ions on the surface of the phospholipid bilayer, we utilized synthetic lipids with DTPA chelating groups attached to the region of polar head. Incorporating such lipids in a phospholipid bilayer allows us to bind Gd^{3+} ions to the known positions with respect to the membrane surface. To develop a spectroscopic ruler, we have used spin-labeled phospholipids. By "moving" the attachment position of the nitroxide along the lipid chain, samples with varying lengths of nitroxide-gadolinium interspin vectors could be prepared.

3.2.1 Sample Preparation

DMPC/ cholesterol (30 mole%) bilayer containing only 1 mole% of DMPE-DTPA (1,2-Dimyristoyl-*sn*-Glycero-3-Phospho Ethanolamine DiethyleneTriaminePentaAcetate)

samples was prepared. Samples were labeled with 5, 7, 10, 12, and 16-doxyl-labeled lipids as well as cholestane spin label at concentration 1 mole%. Samples were prepared by mixing required amounts of chloroform solutions of DMPC, cholesterol, DMPE-DTPA and spin-labeled lipids. Chloroform was evaporated and samples were kept overnight under high vacuum. Required amount of Hepes buffer (pH 7.4) was added and the suspension was treated with 10 freeze-thaw cycles to make liposomes. To label liposomes with metal ions, buffer containing the required amount of gadolinium or lanthanum nitrate was added to the liposome suspension.

X-band and W-band EPR experiments and spectral simulations were carried out as described in Section 3.1.1

3.2.2 Determining Position of Gd^{3+} Ions With Respect to the Bilayer Surface

Effect of Gd^{3+} ions bound to the chelating group on the surface of the bilayer on CW EPR spectra of nitoxide radicals attached to the lipid chains as a function of the nitroxide transmembrane position was investigated. In control experiments, EPR spectra of samples containing nitroxide label and lanthanum ions were obtained at T=77 K. Lanthanum has a very fast electronic relaxation time even at low temperature, and as a result, no line width broadening was observed compared with the samples containing no metal ion. Use of lanthanum in the control experiment was motivated by the fact that addition of metal ion to the liposomes could affect lipid dynamics and bilayer polarity, producing unwanted changes in nitroxide EPR spectra. By comparing spectra from samples containing La and Gd^{3+} only changes induced by metal-nitroxide interaction

would be observed. Addition of Gd^{3+} ion resulted in pronounced broadening of the CW EPR spectra from the nitroxide label. To extract the broadening one-parameter fitting model was used (Equation 19). Spectrum from sample containing La was used as an envelope $F_o(B)$ (the spectrum taken in the absence of broadening agent), and spectrum from the sample containing Gd^{3+} was used as $F(B)$ (spectrum in the presence of a relaxer). Lorentzian was used as broadening function $m(B)$. EPR spectra from Gd^{3+} ions at X-band are very broad, about 300-500 G, and do not interfere with analysis of much narrower nitroxide spectra. Least-squares fitting using one-line width parameter model shows that the broadening is essentially homogeneous, and no changes in hyperfine splitting were observed. The latter indicates that the microenvironment of the labeled site is unaffected by the addition of Gd^{3+} ion. Using samples containing nitroxide labels at positions 5, 7, 10, 12, and 16 along the lipid chain dependence of the induced broadening upon depth of the nitroxide label in the bilayer was investigated. Results are shown in Figure 23. Gd^{3+}-induced broadening decreases progressively as nitroxide label is moved from the polar head region of the bilayer to its center. At T=100 K the broadening is a result of dipole-dipole interactions. By using a model of the paramagnetic relaxer distributed on the liposome surface, the magnitude of the dipole broadening should change as $1/r^4$. From analyses of the data in Figure 24 using this distance dependence one can estimates that the Gd^{3+} ions are located approximately 14 Å away from the membrane surface and in an aqueous phase. This result is consistent with the structure of the chelating group and its attachment to the lipid.

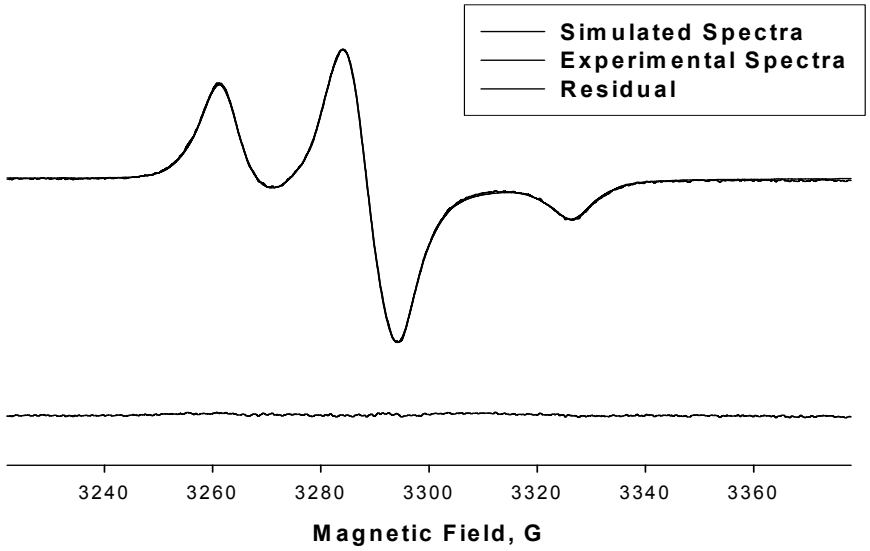

Figure 23: DMPC/DOPG/Cholesterol/10DL EPR X-band Spectra; Broadening = 0.41G

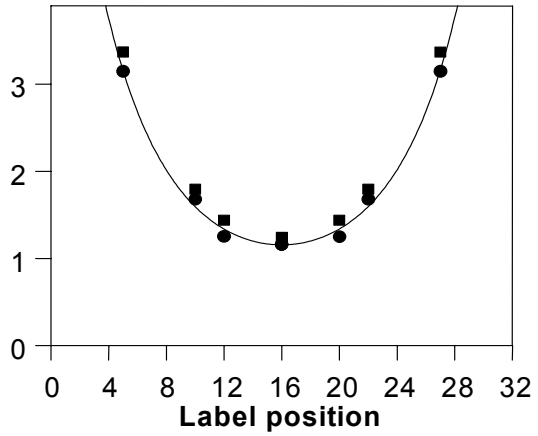

Figure 24: Profiles of Lorentzian broadening induced by Gd-nitroxide spin-spin interactions, T=100 K. Square = fit center line only Circle = fit entire spectrum

3.2.3 Measurements of Gd^{3+}-Induced Nitroxide Relaxation Enhancement Using 95 GHz Spectrometer

W-band spectra from liposome samples labeled at various positions along the lipid chain as well as with cholestane (CSL) were obtained at T = 6 ^{0}C. At this temperature EPR spectra from most of these labels fall into a slow motional regime. Changes in EPR spectra upon addition of 1 mM of Gd^{3+} were observed. Figure 25 shows 95 GHz EPR spectrum of DMPC/ Cholesterol/DMPE-DTPA labeled with cholestane in the presence of 1mM Gd^{3+}. At this Gd^{3+} concentration, only one out of three chelating groups contains the Gd^{3+} ion, ensuring that there is no non-specific binding of metal ion to the polar phospholipid head group. Figure 26 clearly shows complete separation of nitroxide and Gd^{3+} EPR spectra. Also, it demonstrates that at 95 GHz all three principal axis components of g-tensor (labeled as g_x, g_y and g_z) are spectrally resolved, allowing analysis of anisotropy of Gd^{3+}-nitroxide interactions.

Figure 27 shows a 95 GHz EPR spectrum of 5-doxyl-labeled DMPC/cholesterol/DMPE-DTPA/La bilayer at T = 6 ^{o}C superimposed with the spectrum from the same system labeled with Gd^{3+}. It is clear that z-component of the spectrum is unaffected by the interaction with Gd^{3+}, while intensities of the x- and y-components are reduced.

Anisotropic interactions were observed for samples labeled with the cholestane spin-label (CSL). CSL is a nitroxide-containing cholesterol analogue that inserts into the bilayer with the nitroxide moiety in the region of the lipid polar heads. Figure 26 shows experimental 95 GHz (X-band) EPR spectrum of DMPC/ Cholesterol/DMPE-DTPA labeled with cholestane, superimposed with spectrum from the same system in presence

of Gd^{3+} ions. For CSL interaction with Gd^{3+} reduces spectral amplitude of x- and z-components leaving the y-component unchanged.

To understand the observed changes in the spectra for 5-doxyl lipid and CSL orientation of those molecules with respect to the bilayer surface has to be considered. 5-doxyl-labeled lipid is incorporated into the bilayer such that the positioning of the doxyl moiety points its z-magnetic axis essentially along the lipid chain (i.e. normal to the membrane surface). For the cholestane label, the nitroxide y-axis is oriented along the lipid chain and is normal to the bilayer surface. This orientation is reflected in the spectral changes observed for 5-doxyl-lipid and CSL signals. Observed anisotropy of spectral changes holds a promise that in high field EPR experiments, orientation of the nitroxide label attached to the protein side chain with respect to the membrane surface can be determined. Such experiments would be absolutely unique since orientational information could be obtained from microscopically disordered samples at physiologically relevant conditions.

Analysis of the spectral changes will require utilization of the Leigh approach extended to the case of anisotropic interaction and will provide distance measurements between the surface of the membrane and position of the nitroxide label. This task is beyond of the scope of this project.

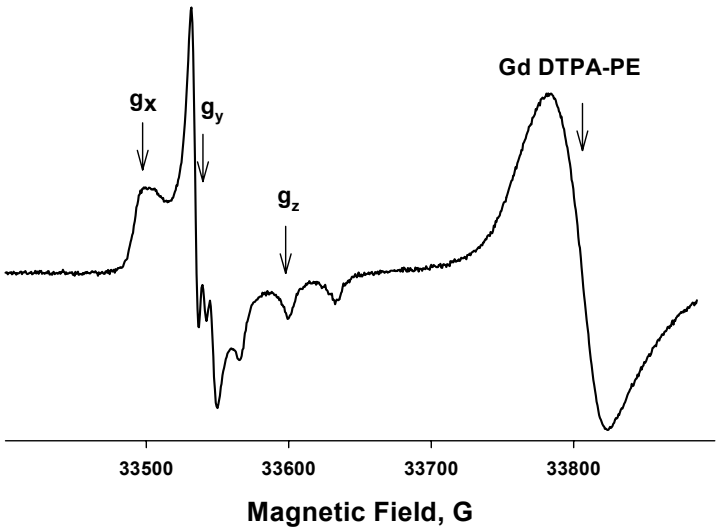

Figure 25: HF EPR spectrum (95GHz) of DMPC/Cholesterol/DMPE-DTPA/cholestane with 1mM Gd^{3+} showing complete separation of nitroxide and Gd^{3+}spectra

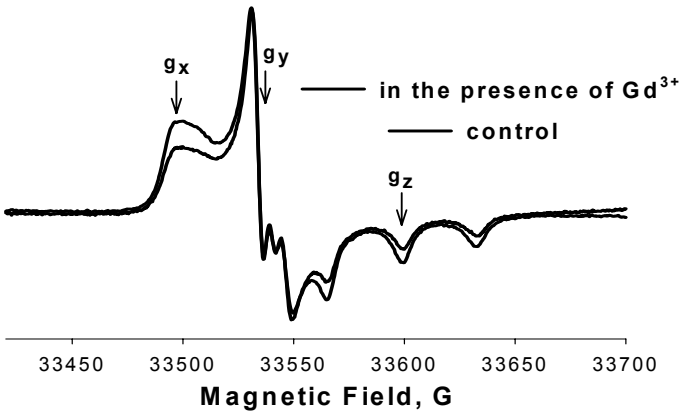

Figure 26: HF EPR spectrum (95GHz) of CSL (y-probe). g_y component of the spectrum is unaffected by dipolar interaction

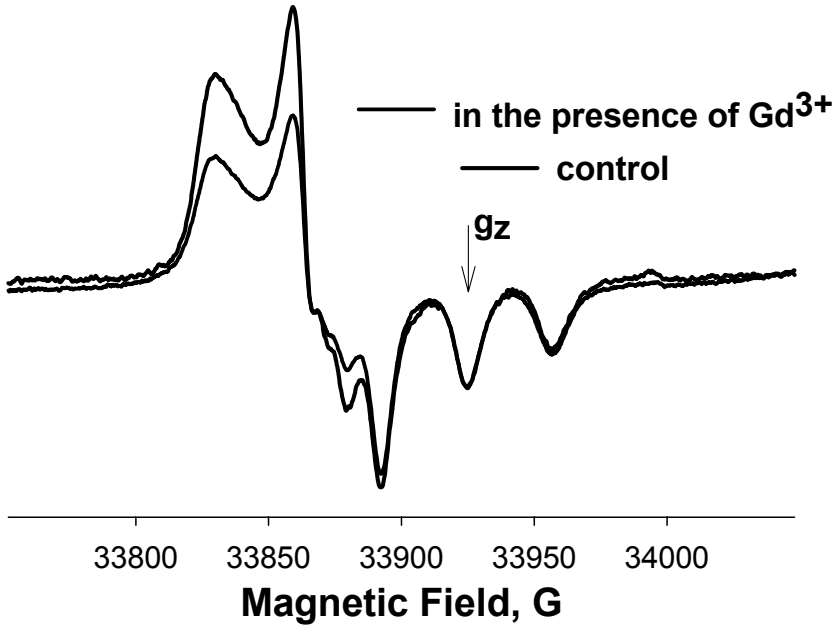

Figure 27: HF EPR spectrum (95GHz) of 5-doxyl-PC (z-probe). g_Z component of the spectrum is unaffected by dipolar interaction

3.3 Conclusions

In the work reported here we have accomplished a number of goals: we now understand the nature of the interaction of Gd^{3+} ions with nitroxide radicals in moderately viscous solutions.

We have shown that:

1. In systems studied, the Heisenberg spin exchange contribution to nitroxide line width broadening by Gd^{3+} complexes is negligibly small when compared with the dipole-dipole contribution, so the dipolar theory could be used for distance determination without corrections for exchange.

a. Nitroxide-Gd^{3+} dipole-dipole interaction under conditions studied is modulated by the spin-lattice T_{1e} electronic relaxation of Gd^{3+}.

b. Magnetic field dependence of T_{1e} electronic relaxation of Gd^{3+} could be used to increase the magnitude of Gd^{3+}-induced line width broadening. This means that longer interspin distances could be measured at higher magnetic fields.

2. We have shown the feasibility of novel spin-labeling approach for membrane studies based on Gd^{3+}-nitroxide pairs:

a. We have developed a methodology to position Gd^{3+} ions on the surface of the phospholipid bilayer using chelating lipids and have determine the exact location of the Gd^{3+}ions in DMPC/cholesterol/DMPE-DTPA bilayers.

b. We have shown that at high magnetic field (W-band experiment) such a labeling method has a potential to provide both, distance between nitroxide label and the surface of the bilayer and orientation of the nitroxide with respect to the surface.

4 REFERENCES

1. Yeagle, P. and Lee, A. (2002) "Membrane protein structure," *Biochim. Biophys. Acta*., **1565**, 143-146.

2. Palczewski, K., Kumasaka, T., Hori, T., Behnke, C., Motoshima, H., Fox, B., Le Trong, I., Teller, D., Okada, T., Stenkamp, R. (2000) "Crystal structure of rhodopsin: a G protein-coupled receptor," *Science*, **289**:739-745.

3. Okada, T., Le Trong, I., Fox, B., Behnke, C., Stenkamp, R., Palczewski, K. (2000) "X-ray diffraction analysis of three-dimensional crystals of bovine rhodopsin obtained from mixed micelles," *J. Struct. Biol.*, **130**:73-80.

4. Kolbe, M., Besir, H., Essen, L., Oesterhelt, D. (2000) "Structure of the light-driven chloride pump halorhodopsin at 1.8A resolution," *Science*, **288**:1390-1396.

5. Opella, S., Ma, C., Marassi, F. (2001) "Nuclear magnetic resonance of membrane-associated peptides and proteins," *Methods Enzymol* , **339**:285-313.

6. Hubbell, W. and Altenbach, C. (1994) *Curr. Opin. Struct. Biol*., **4**, 566-573.

7. Voss, J.,Salwinski, L., Kaback, H., and Hubbell, W. (1995) "A method for distance determination in proteins using a designed metal ion binding site and site-directed spin labeling: Evaluation with T4 lysozyme," *Proc. Natl. Acad. Sci. USA*, **92**, 12295.

8. Altenbach, C., Oh, K., Trabanino, R., Hideg, K., Hubbell, W. (2001) "Estimation of inter-residue distances in spin labeled proteins at physiological temperatures: experimental strategies and practical limitations," *Biochemistry*, **40**, 15471.

9. Bender, C. and Berliner, L. *Biological Magnetic Resonance, Volume 19: Distance Measurements in Biological Systems by EPR*. Kluwer Academic/Pleunm Publishers, (2000).

10. Rabenstein, M. and Shin, Y. (1995) "Determination of the distance between two spin labels attached to a macromolecule," *Proc. Natl. Acad. Sci. USA*, **92**, 8239.

11. Likhtenshtein, G. and Bobodzhanov, P. (1968) "Investigation of the structure and local conformational transitions of proteins and enzymes by the method of double paramagnetic labels," *Biofizika*, **13,** 757-764.

12. Kulikov, A., Likhtenshtein, G. Rozantsev, E., Suskina, V. (1972) "Possibility of determining the distances between the functional groups of protein by the method of paramagnetic labels," *Biofizika*, **17,** 42-48.

13. Leigh, J. (1970) "ESR rigid-lattice line shape in a system of two interacting spins," *J. Chem. Phys*. **52**, 2608-2612.

14. Voss, J., Wu, J., Hubbell, W., Jacques, V., Meares, C., Kaback, H. (2001) "Helix packing in the lactose permease of *escherichia coli*: distances between site-directed nitroxides and a lanthanide," *Biochemistry*, **40**, 3184-3188.

15. Harris, R. *Nuclear Magnetic Resonance Spectroscopy: A Physiochemical View*. Longman Group, (1986).

16. Altenbach, C., Greenhalgh, D., Khorana, H., Hubbell, W., (1994) "A collision gradient method to determine the immersion depth of nitroxides in lipid bilayers: application to spin-labeled mutants of bacteriorhodopsin," *Proc. Natl. Acad. Sci*., **91**, 1667-1671.

17. Fajer, P. *ESR Spectroscopy Labeling in Peptide and Protein Analysis.* Meyers (Ed.) (2000).

18. Altenbach, C., Yang, K., Farrens, D., Farahbakhsh, Z, Khorana, H., Hubbell, W., (1996) "Structural features and light-dependent changes in the cytoplasmic interhelical e-f loop region of rhodopsin: a site-directed spin-labeling study," *Biochemistry*, **35**, 12470-12478.

19. Gross, A., Hubbell, W., (2002) "Identification of protein side chains near the membrane-aqueous interface: a site-directed spin labeling study of KcsA," *Biochemistry*, **41**, 1123-1128.

20. Powell, D., Merbach, A., Gonzales, G., Brucher, E., Micskei, K., Ottaviani, M., Kohler, K., von Zelewsky, A., Grinberg, O., Lebedev, Y. (1993) "Magnetic-field-dependent electronic relaxation of Gd^{3+} in aqueous solutions of the complexes $[Gd(H_20)8]^{3+}$, [Gd(propane-1,3-diamine-N,N,N',N'-tetraacetate)$(H_20)_2$], and [Gd(N,N'-bis[N-methylcarbamoyl])methyl-3-azapentane-1,5-diamine-3,N,N'-triacetate)(H_20)] of interest in magnetic resonance imaging", *Helv. Chem. Acta*, **76**, 2129-2146.

21. Bender, C. and Berliner, L. *EPR: Instrumental Methods: Biological Magnetic Resonance, Volume 21: Distance Measurements in Biological Systems by EPR*. Kluwer Academic/Pleunm Publishers, (2004).

22. Atsarkin, V., Demidov, V., Vasneva, G., Odintsov, B., Belford, R., Raduchel, B., Clarkson, R. (2001) "Direct measurement of fast electron spin-lattice relaxation: method and application to nitroxide radical solutions and Gd3+ contrast agents," *J. Phys. Chem. A.*, **105**, 9323-9327.

23. Smirnova, T., Smirnov, A., Belford, R., Clarkson, R. (1998) "Lipid magnetic resonance imaging contrast agent interactions: a spin-labeling and a multifrequency EPR study," *J. Am. Chem. Soc*., **120**, 5060-5072.

24. Smirnova, T., Smirnov, A., Belford, R., Clarkson, R. (1995) “W-band (95 GHz) EPR spectroscopy of nitroxide radicals with complex proton hyperfine structure: fast motion,” *J. Phys. Chem*., **99**, 9008-9016.

25. Kowert, B. (1981) “Determination of the anisotropic and nonsecular contributions to ESR line widths in liquids,” *J. Phys. Chem*., **85**, 229-235.

26. Budil, D., Earle, K., Freed, J. (1993) “Full determination of the rotational diffusion tensor by EPR at 250 GHz,” *J. Phys. Chem*., **97**, 1294-1303.